



University of  
Massachusetts  
Amherst

## Urban Air Pollution and Climate Stressors: Exploring Nitrogen Dioxide Patterns and Heat Wave Impacts in Holyoke, MA

Item Type	Thesis (Open Access)
Authors	Beltran Vargas, Nathalie
DOI	<a href="https://doi.org/10.7275/55870">10.7275/55870</a>
Rights	Attribution-NonCommercial 4.0 International
Download date	2026-05-11 03:01:58
Item License	<a href="http://creativecommons.org/licenses/by-nc/4.0/">http://creativecommons.org/licenses/by-nc/4.0/</a>
Link to Item	<a href="https://hdl.handle.net/20.500.14394/55870">https://hdl.handle.net/20.500.14394/55870</a>

Urban Air Pollution and Climate Stressors: Exploring Nitrogen Dioxide Patterns and Heat Wave  
Impacts in Holyoke, MA

A Thesis Presented

By

Nathalie Beltran Vargas

Submitted to the Graduate School of the  
University of Massachusetts Amherst in partial fulfillment  
of the requirements for the degree of

MASTER OF SCIENCE

February 2025

Master of Science in Environmental Health

Urban Air Pollution and Climate Stressors: Exploring Nitrogen Dioxide Patterns and Heat Wave  
Impacts in Holyoke, MA

A

Thesis Presented

By

NATHALIE BELTRAN VARGAS

Approved as to style and content by:

---

Raphael Arku, Chair

---

Laura L. Figueroa, Chair

---

Richard Peltier, Member

---

Song Liang, Chair  
Department of Environmental Health Sciences

## ACKNOWLEDGMENTS

I would like to begin by expressing my heartfelt gratitude to God and my church members for their unwavering support, which has been instrumental in helping me complete my master's thesis program. I extend my deepest thanks to my thesis advisors, Dr. Raphael Arku, Dr. Laura Figueroa, and Dr. Rick Peltier, for their invaluable guidance, mentorship, and encouragement throughout this journey. Their expertise and insights have been pivotal in shaping my academic growth and the completion of this thesis.

I am also profoundly grateful to the members of the Arku and Figueroa labs for their assistance and encouragement during this process. A special thanks to Carissa Lange, Barbara E. Mottey, and Grace Shiffrin for their support, time, and dedication, which were vital to my success. Furthermore, I wish to express my sincere gratitude to the JPB Foundation through Harvard's Environmental Health Program, Holyoke Community College, and Nuestras Raíces for their collaboration and generous support.

Lastly, but certainly not least, I extend my deepest appreciation to my husband, family, and friends outside of UMASS for their emotional support and love, which have been a constant source of strength and motivation.

## ABSTRACT

### URBAN AIR POLLUTION AND CLIMATE STRESSORS: EXPLORING NITROGEN DIOXIDE PATTERNS AND HEAT WAVE IMPACTS IN HOLYOKE, MA

FEBRUARY 2025

NATHALIE BELTRAN VARGAS, B.A., SPRINGFIELD COLLEGE

M.A., UNIVERSITY OF MASSACHUSETTS AMHERST

**Directed by: Raphael Arku**  
**Directed by: Laura L. Figueroa**

Climate change and air pollution are interconnected, with nitrogen dioxide (NO<sub>2</sub>) and heatwaves intensifying in urban environments, exacerbating public health risks and impacting urban agriculture. Therefore, we aimed to conduct a city-wide year-long measurement campaign to understand the spatiotemporal patterns and concentrations of NO<sub>2</sub>. Also, we aimed to assess the impact of heatwave exposure during early plant development on plant growth, phenology, flowering, fruit production, and the abundance of floral and non-floral visitors. We measured ambient NO<sub>2</sub> concentrations in Holyoke, MA, from August 2021 to 2022, using Ogawa passive samplers. We collected 260 weekly NO<sub>2</sub> samples at 25 sites classified based on their land use characteristics. Sites included ‘fixed’ (yearlong, n = 5) and ‘rotating’ (weeklong, n = 20) locations. Results showed higher NO<sub>2</sub> concentrations during winter (>150 µg/m<sup>3</sup>) compared to summer (<3.4 µg/m<sup>3</sup>), with commercial and highly dense sites experiencing the highest mean concentrations (17.09 µg/m<sup>3</sup>). Approximately 61% of rotating sites and 62% of weekly samples from fixed sites exceeded WHO air quality guidelines. A mixed-effects model revealed that weekly mean temperature, NDVI, and wind speed were the strongest predictors of NO<sub>2</sub>. Additionally, we investigated the effects of heatwaves in urban environments using cherry tomato plants as a model system. Plants (n = 96) were exposed to heatwave (HW:37.7°C) and

control (C: 28.8°C) conditions for 3 days during early development, then transplanted to pots and moved to 3 sites. We performed various surveys to assess plant growth, flowering, phenology, fruit production, and floral and non-floral visitors' abundance. Heatwave exposure increased total flower counts yet did not influence initial growth rate or weekly plant height, but when the site with additional nutrient access was excluded, HW exposure significantly reduced plant height. HW-exposed plants produced more mature and immature fruits, attracted more non-floral visitors, and led to a delay in fruit ripening time. These findings highlight the dual challenges of air pollution and climate stressors in urban environments, emphasizing the need to understand their interactions to protect public health and support urban agriculture.

# Table of Contents

<b>ACKNOWLEDGMENTS</b> .....	<b>iii</b>
<b>ABSTRACT</b> .....	<b>iv</b>
<b>List of Tables</b> .....	<b>viii</b>
<b>List of Figures</b> .....	<b>ix</b>
<b>CHAPTER 1</b> .....	<b>10</b>
<b>1.1.1 INTRODUCTION</b> .....	<b>10</b>
1.1.2 Health effects associated with nitrogen dioxide (NO <sub>2</sub> ).....	10
1.1.3 Disparities in nitrogen dioxide (NO <sub>2</sub> ) exposure .....	13
1.1.4 Air Quality in Massachusetts .....	13
<b>1.2.1 METHODS</b> .....	<b>16</b>
1.2.2 Study Location .....	16
1.2.3 Study Design.....	18
1.2.4 Nitrogen dioxide (NO <sub>2</sub> ) measurement and analytical methods.....	19
1.2.5 Data management and statistical analysis.....	20
1.2.6 Determinants of NO <sub>2</sub> concentration in Holyoke .....	22
1.2.7 Model development .....	24
<b>1.3.1 RESULTS</b> .....	<b>25</b>
1.3.2 Spatial patterns.....	25
1.3.3 Temporal Patterns.....	27
1.3.4 Seasonal Patterns .....	28
1.3.5 Mixed Effect Model Results .....	29
<b>1.4.1 DISCUSSION</b> .....	<b>30</b>
1.4.2 Strengths and Limitations of the Study .....	34
1.4.3 Conclusion .....	35
<b>CHAPTER 2</b> .....	<b>36</b>
<b>2.1.1 INTRODUCTION</b> .....	<b>36</b>
<b>2.2.1 METHODS</b> .....	<b>39</b>
2.2.2 Plant Model .....	39
2.2.3 Experimental Heatwave Exposure .....	40
2.2.4 Site Selection and Field Season Duration .....	41
2.2.5 Plant Growth and Phenology Surveys .....	42
2.2.6 Floral and Non-floral Visitor Surveys .....	43
<b>2.3.1 STATISTICAL ANALYSIS</b> .....	<b>44</b>
2.3.2 Applications, Software, and Packages .....	44
2.3.3 Statistical analysis applied to models .....	48
2.3.4 Statistical Evaluation of Models Excluding Youth Garden.....	49
<b>2.4.1 RESULTS</b> .....	<b>49</b>
2.4.2 Plant Growth .....	49
2.4.3 Flower and Fruit Phenology.....	50
2.4.4 Flower Count .....	51
2.4.5 Fruit Production.....	53
2.4.6 Abundance of Floral Visitors.....	54

2.4.7 Non-floral Visitor Abundance .....	56
<b>2.5.1 DISCUSSION .....</b>	<b>57</b>
2.5.2 Strengths and Limitations of the Study .....	62
<b><i>Supplementary Text</i> .....</b>	<b>64</b>
<b>REFERENCES .....</b>	<b>66</b>

## List of Tables

Table 1. Description of candidate spatial predictor variables.....	23
Table 2. Mean and standard deviation (SD) by site type.....	26
Table 3. Mean association of log NO <sub>2</sub> with spatial predictor variables in the final model .....	29
Table 4. Plant model summaries.....	45
Table 5. Floral and non-floral visitor models summary .....	48

## List of Figures

Figure 1. Map of Holyoke, MA .....	16
Figure 2. R-squared values .....	24
Figure 3. Histogram of unlogged and logged nitrogen dioxide (NO <sub>2</sub> ) concentrations.....	25
Figure 4. Seasonally adjusted weekly NO <sub>2</sub> concentrations for rotating sites .....	26
Figure 5. Box plot of the distribution of NO <sub>2</sub> at the fixed sites .....	27
Figure 6. Seasonal variation of NO <sub>2</sub> concentrations at the fixed sites.....	28
Figure 7. Sampling sites.....	41
Figure 8. Box plot of plant growth and height.....	50
Figure 9. Plant and fruit phenology box plots.....	51
Figure 10. Box plot of number of flowers .....	52
Figure 11. Box plots of fruit production .....	54
Figure 12. Bar plots of floral and non-floral visitors .....	55

## CHAPTER 1

### 1.1.1 INTRODUCTION

#### 1.1.2 Health effects associated with nitrogen dioxide (NO<sub>2</sub>)

Air pollution is a major environmental and public health concern worldwide. Both ambient and household air pollution are associated with 6.7 million premature deaths, annually (World Health Organization [WHO], 2022). Most of the deaths are from cardiovascular and respiratory diseases (Jiang et al., 2016). In addition to the cardiovascular and respiratory systems, air pollution has been shown to impact nearly every organ in the human body, from adverse birth outcomes to neurodegenerative conditions (Dominski et al., 2021). Most of the current global burden of air pollution is borne by low- and middle-income countries, where air pollution levels remain detrimentally high (George et al., 2023).

In high-income countries, urban air pollution is a significant environmental health risk factor for city dwellers. Major sources of urban air pollution include traffic emissions, residential heating, dust from construction and roadways, and industrial activities (Hoffman et al., 2019). Consequently, six key air pollutants—carbon monoxide (CO), lead (Pb), nitrogen dioxide (NO<sub>2</sub>), ozone (O<sub>3</sub>), particulate matter (PM<sub>2.5</sub> and PM<sub>10</sub>), and sulfur dioxide (SO<sub>2</sub>) — are carefully regulated and monitored. Since the establishment of the Clean Air Act in the 1970s, the federal law that regulates air emissions, the United States has achieved significant reductions in all criteria air pollutants, even alongside economic growth reflected in the rising gross domestic product (U.S. Environmental Protection Agency [EPA], 2011). However, these improvements do not eliminate the potential for adverse health outcomes, as health issues related to air pollution

exposure still occur in urban areas (Mananga et al., 2024). Therefore, it is crucial to continue to investigate how human health is affected by air pollutants.

Besides fine particulate matter (PM<sub>2.5</sub>), nitrogen dioxide (NO<sub>2</sub>) is the most common urban air pollutant studied. NO<sub>2</sub> results from the oxidation of nitric oxide and is part of a group of very reactive gases called nitrogen oxides (NO<sub>x</sub>), which are composed of nitrogen and oxygen molecules and include nitric oxide, nitrogen monoxide, nitrous oxide, nitrogen trioxide, and nitrogen pentoxide. As a byproduct of combustion, NO<sub>2</sub> pollution is produced by the combustion of automobiles and power plants and the burning of fuels at very high temperatures. During fuel combustion, nitrogen and oxygen combine at high temperatures to form nitric oxide (NO), which converts to nitrogen dioxide (NO<sub>2</sub>). Compared to other criteria pollutants, NO<sub>2</sub> has a shorter lifetime and more spatial heterogeneity, where the concentrations can vary significantly from one location to the other, depending on the sources. While NO<sub>2</sub> can also come from naturally occurring sources (e.g. volcanic eruptions, and forest fires), ~70% of all emissions can be linked to anthropogenic sources (Boningari & Smirniotis, 2016, Salonen et al., 2019). In the atmosphere, NO<sub>2</sub> can react with other chemicals to produce secondary pollutants like ozone and acid rain (EPA, 2023). Also, it is important to recognize that NO<sub>2</sub> is an indicator species for other pollutants that are equally harmful. For example, sources that emit NO<sub>2</sub> during combustion processes from vehicles, power plants, and heating systems, can also emit other pollutants such as PM, CO, SO<sub>2</sub>, and volatile organic compounds (VOCs)(Matthaios et al., 2023; Bozkurt et al., 2018).

With low solubility in water, NO<sub>2</sub> can penetrate deep into the respiratory system, where it can diffuse through alveolar cells and capillaries, leading to respiratory illnesses. Specifically, NO<sub>2</sub> exposure damages lung tissues by promoting lipid and protein oxidation through free

radical generation, reduces immunity, and impairs infection resistance by altering macrophage function (Boningari & Smirniotis, 2016; Petit et al., 2017). Overall, NO<sub>2</sub> can produce a variety of clinical responses depending on its concentration and duration of exposure (National Academies Press US, 1998).

Long-term exposure to NO<sub>2</sub> has been shown to pose significant health risks. In a meta-analysis, researchers evaluated the association between long-term NO<sub>2</sub> exposure and all-cause, cardiovascular, and respiratory mortality, analyzing 1,349 studies to calculate pooled and subgroup-specific hazard ratios (HRs). They found that each 10 ppb increase in annual NO<sub>2</sub> concentration was associated with a pooled HR of 1.06 for all-cause mortality, 1.11 for respiratory-related mortality, and 1.05 for cardiovascular mortality (Huang et al., 2021). This analysis indicates that long-term NO<sub>2</sub> exposure increases mortality risk from various causes independent of other common air pollutants. However, the adverse health effects of NO<sub>2</sub> exposure are not limited to long-term exposure but are also present in the short term.

Another group of researchers conducted a systematic review to assess the link between short-term NO<sub>2</sub> exposure and daily mortality, calculating random effects estimates across different continents and globally. Their findings showed a positive association between NO<sub>2</sub> and both all-cause and cause-specific mortality. Specifically, a 10 ppb increase in NO<sub>2</sub> was associated with a 1.58% rise in all-cause mortality, a 1.72% increase in cardiovascular mortality, and a 2.05% increase in respiratory mortality (Wang et al., 2021). Additional research has demonstrated a connection between short-term NO<sub>2</sub> exposure and emergency department visits for respiratory diseases in children, a population particularly vulnerable to air pollution. For example, a study in China found that short-term NO<sub>2</sub> exposure was associated with increased emergency visits for respiratory illnesses, particularly acute upper respiratory infections in

children aged 0–5, as well as conditions like bronchitis and pneumonia (He et al., 2022). These findings highlight the significant impact of NO<sub>2</sub> exposure on both short- and long-term health, emphasizing the need for measures to reduce NO<sub>2</sub> levels and protect public health.

### **1.1.3 Disparities in nitrogen dioxide (NO<sub>2</sub>) exposure**

Multiple studies have shown the disparities in exposure to multiple air pollutants, including NO<sub>2</sub>, across marginalized communities in the US (Cheesman et al., 2022; Clark et al., 2014; Wang et al., 2023). Wang et al. (2023) found that while there has been a significant decrease in the outdoor concentrations of NO<sub>2</sub> over time, racial and ethnic minorities are disproportionately exposed to higher concentrations in comparison to the white population. These inequities have persisted, and some have worsened over time. For example, a study revealed that Black, Hispanic, Asian, and multiracial populations experience 15-50% higher concentrations of NO<sub>2</sub> than the national average, while non-Hispanic whites experience 5-15% lower concentrations (Hunter et al., 2023). Another study that investigated socioeconomic disparities in air quality at public schools in the US found that schools with a higher proportion of marginalized students living in poverty experienced higher concentrations of NO<sub>2</sub> and PM<sub>2.5</sub> than those schools with a lower proportion of marginalized students (Chessman et al., 2022). The disproportionate exposure to this hazardous pollutant poses serious health risks to low-income and marginalized communities, underscoring the need to continue our efforts to understand NO<sub>2</sub> sources, identify areas with the highest concentrations, and develop models to predict exposures in areas where monitoring data remains sparse.

### **1.1.4 Air Quality in Massachusetts**

One of the Clean Air Act requirements was the establishment of the National Ambient Air Quality Standards (NAAQS) for common air pollutants (criteria air pollutants). These

pollutants are carbon monoxide (CO), nitrogen dioxide (NO<sub>2</sub>), ozone (O<sub>3</sub>) particles (PM<sub>10</sub> and PM<sub>2.5</sub>), and sulfur dioxide (SO<sub>2</sub>) ([NAAQS Table | US EPA, 2024b](#)). These standards provide public health protection for the general population, including protecting the health of sensitive groups such as asthmatics, children, and the elderly (EPA). Between 1970 and 2020, combined emissions of these criteria pollutants dropped by 78%, with many cities and states enjoying improved air quality and attaining the NAAQS across the country (EPA, 2022). The CAA requires each state to monitor outdoor air quality and develop and implement a plan to ensure that all areas of the state maintain federal standards. In addition to the EPA's air quality standards, there is also the World Health Organization (WHO) air quality guidelines (AQGs), which provide evidence-based recommendations for pollutant concentration limits aimed at achieving cleaner air and safeguarding public health. Although the WHO air quality guidelines are not legally enforced, they guide national governments across the world to develop policies to reduce the population's exposure to air pollution.

The Massachusetts Department of Environmental Protection (MassDEP) has more than twenty monitoring stations, where they forecast for ozone and particulates and collect data on other criteria air pollutants. Based on its 2022 Air Quality Report, Massachusetts met the air quality standards for all criteria pollutants, indicating that monitored pollutant levels across the state remained within the allowable limits for that year. There were only four days in which ozone concentrations exceeded the 8-hour national standard of 0.070 parts per billion (ppm) or 70 µg/m<sup>3</sup> but not the WHO AQG of 100 µg/m<sup>3</sup>. This is likely due to the state's use of fossil fuels for heating, transport, and electricity, as fossil fuels are the primary source of air pollution in Massachusetts (Landrigan et al., 2022). Despite the over-high quality of the state's air quality,

there are smaller environmental justice cities currently facing issues with air pollution (McIntyre et al., 2024).

In 2019, air pollution was responsible for an estimated 2,780 deaths in MA. Among these deaths, approximately 1,677 were due to cardiovascular disease, 2,185 to lung cancer, 200 to stroke, and 343 were related to respiratory diseases (Landrigan et al., 2022). It is important to note that some deaths may be associated with multiple conditions. Therefore, the sum of cause-specific estimates exceeds the total number of deaths. In addition, studies of traffic-related air pollution across the state suggest that prenatal exposure can increase the risk of birth defects and gestational diabetes mellitus while also resulting in smaller ultrasound biometric parameters (e.g., fetal growth, head, and abdominal circumference, femur length, and biparietal diameter) (Girguis et al., 2015; Fleisch et al., 2016; Gao et al., 2023).

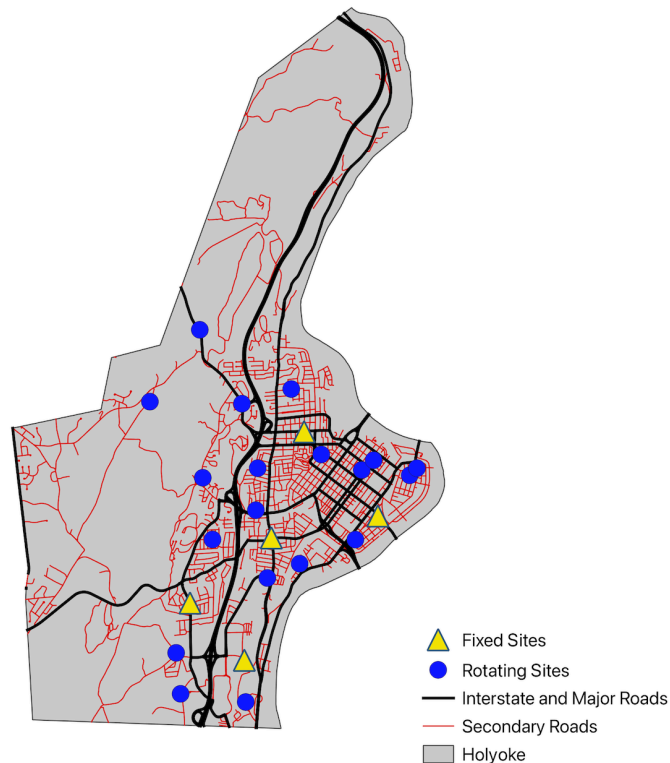
Furthermore, disparities in air pollution exposure have been identified in MA. For example, Rosofsky and colleagues quantified inequality by modeling  $PM_{2.5}$  and  $NO_2$  concentrations across the entire state and comparing those concentrations to race, ethnicity, income, and education composition. By doing so, the researchers were able to identify the populations most vulnerable to air pollution exposure. In general, they found that air pollution inequalities exist, particularly, in urban areas and among the Hispanic population. Thus, the results suggest that further research efforts should focus attention on these communities. Therefore, the primary objective of this chapter is to examine the spatiotemporal distribution of  $NO_2$  concentrations in Holyoke, MA—a city largely composed of marginalized communities, primarily Hispanics. It also seeks to develop a predictive model to identify factors influencing these concentrations, with the ultimate goal of informing strategies to protect Holyoke residents from the effects of air pollution.

## 1.2.1 METHODS

### 1.2.2 Study Location

Our study was conducted in the city of Holyoke, MA (Figure 1). Holyoke is part of Hampden County in Massachusetts, located East of the Mount Tom Range, and home to the Barnes Aquifer, a major regional environmental resource. In addition, Holyoke is recognized for being one of the first planned industrial cities in the world (Smith et al., 2013). During the 19<sup>th</sup> and 20<sup>th</sup> centuries, Holyoke, nicknamed the “Paper City,” was the world’s leading paper producer. At this time, approximately 25 companies were producing various paper materials throughout the city. At the same time, multiple textile mills also contributed to the city’s economy (Strahan, 2019).

Figure 1. Map of Holyoke, MA



Map of Holyoke, MA, indicating the location of fixed and rotating sites as well as interstates, major roads, and secondary roads.

From the 1960s until 2014, there was a coal-fired power plant located in Holyoke along the Connecticut River. Holyoke still reflects its industrial history through infrastructure such as mills, old paper factories, and housing.

One of the most distinctive characteristics of Holyoke is that its population of 38, 238 is ~51.6% Hispanic. In terms of ethnicities, the population includes white (60.3%), Black or African American (4.2%), two or more races (23.4%), Asian (0.8%), and American Indian and Alaska Native (0.6%) (U.S. Census Bureau). The majority of Hispanic residents identify as Puerto Rican, which is one of the largest Latino groups living in MA. Approximately 25% of the state's Puerto Rican residents live in Holyoke and Springfield (a large metropolis located several miles south of Holyoke) (Granberry et al., 2020). Puerto Ricans began arriving in the region due to the agricultural need during World War II and the Jones Act of 1917, which granted Puerto Ricans citizenship (Granberry et al., 2020). This mass migration has helped shape the city's social, economic, and demographic qualities, all of which should be considered when investigating health outcomes associated with air pollution (Clark et al., 2014).

In addition to having a large Hispanic population, 45.1% of Holyoke residents report speaking a language other than English. Though nearly 80% of the population reports having graduated from high school, only 20% have a bachelor's degree or higher, compared to the national average of 34.2% (U.S. Census Bureau). Holyoke is also a city with a high poverty rate and a low median household income of \$45,045, with an estimated 26.5% of the population living in poverty. With a total of 15,062 houses and ~2.48 people per household (U.S. Census Bureau), most of the residents live in the old housing stock. The sociodemographic characteristics of Holyoke are key to the understanding of how air pollution and race, ethnicity, and financial stability play a role in the concentrations of NO<sub>2</sub> that people experience. This is

because communities where people have a lower socioeconomic status are unequally affected by air pollution and are more susceptible to the effects of various pollutants because of access-related disparities (Clark et al., 2023).

According to the Massachusetts Association of Community Development Corporations (MACDC), the annual average age-adjusted rates of hospital admissions and emergency department visits for asthma are 2-4 times higher for the City of Holyoke, Springfield, and Brockton than across the state (cite). Additionally, the 2021 Massachusetts Department of Public Health Annual Childhood Lead Poisoning Surveillance Report demonstrated that emergency visits due to asthma per 10,000 people are around 4.5 times higher for Blacks (132.8) and Hispanics or Latinos (142.4) than whites (29.5). Despite evidence of the disproportionate impact of air pollution among these groups, only a few programs in Western MA focus on poor air quality. Given the inequitable burden of asthma and the low number of programs focusing on poor air quality, focusing on reducing air pollution may be more sustainable than relying solely on asthma care services after disease onset.

### **1.2.3 Study Design**

We conducted a city-wide year-long measurement for multiple air pollutants, including NO<sub>2</sub>, to develop high-resolution spatial models to predict concentrations of these pollutants across the entire city of Holyoke. Field measurements occurred between August 2021 and August 2022. Weekly integrated NO<sub>2</sub> were collected at yearlong ‘fixed’ (n = 5) and weeklong ‘rotating’ (n = 25) sites (Figure 1). Sampling using a combination of fixed and rotating sites allowed us to capture temporal (annual and seasonal) and spatial (geographic) variations in the measured data. Sites were selected to represent different land use and source features of the city, including geography, population density, road networks and traffic, neighborhoods, and the various

industries. Before field deployment, the team secured approval from the mayor, health director, housing authority, and multiple landlords following discussion of the purposes and goals of the project. The rotating sites were operated in groups of five each week.

#### **1.2.4 Nitrogen dioxide (NO<sub>2</sub>) measurement and analytical methods**

Ogawa passive samplers were deployed to measure NO<sub>2</sub> concentrations. The Ogawa samplers are cost-effective monitoring devices equipped with dual-inlet gas collection pads, coated to chemically react with target gases including NO, NO<sub>2</sub>, SO<sub>2</sub>, and O<sub>3</sub>. After exposure, the collected pads are analyzed in the laboratory to determine the average gas concentrations over the sampling period. Before deployment, the Ogawa samplers were carefully prepared by following the established protocol (Ogawa & Co., Inc., USA). The samples were first cleaned and preloaded in the laboratory and transported to the field in an airtight container to prevent contamination. After the sampling, the samplers were resealed following the same cleaning and handling procedures and transported in airtight vials. In the laboratory, the samples were stored at 4°C until analysis.

To analyze the samples, Ogawa's analytical protocol was followed, where the following reagents were utilized: sulfanilamide solution, NEDA solution, color-producing reagent, nitrate standard stock solution, and Nitrite working standard solution. Samples were extracted using milli-Q-water and then, a color-producing reagent was added. Samples were then equilibrated at room temperature for approximately 20 minutes. The amount of colored derivative produced was determined by a spectrophotometer at a wavelength of 545 nm. Samples were measured three times to ensure precision, and the average was taken to calculate the final concentrations. The sampling time and total concentrations were used to calculate a linear calibration line from a nitrite standard solution. The calibration line was corrected for temperature and relative

humidity. After the absorbance was obtained, the solution concentration was calculated by taking the absorbance and dividing it by the slope of the standard curve. Then, the collected weight was calculated by taking the solution concentration and multiplying it by the volume and 1,000 (factor to convert PPM to PPB). Lastly, the concentrations of NO<sub>2</sub> were calculated by multiplying the concentration conversion coefficient ( $\alpha_{\text{NO}_2}$ ) by the collected weight and dividing it by the exposure time in minutes.

### **1.2.5 Data management and statistical analysis**

One of the primary goals of this project was to understand how land use factors would be influenced and vary in the community. Therefore, each site (n=25) was classified into one of the three land-use categories: (a) commercial/high-density residential (CHR) – areas with commercial businesses, industrial activities, or government offices along with areas of high-density residential features such as narrow paved or unpaved roads and low socioeconomic status (SES); (b) low-density residential (LD) – areas exhibiting low-density residential features such as high SES, medium to wide roads and sparsely populated; and (c) background (BG) – areas with high green space with little to no direct influence from traffic.

Temporal/seasonal adjustments were conducted for all samples from the rotating sites. This is because samples were collected in groups of five during different months and seasons. This seasonal adjustment was implemented to remove temporal trends in the data and create annual equivalents for comparison across all sites. For each sampling week, a temporal factor (TF) was calculated as the ratio of the weekly mean value to the annual mean at all fixed sites.

Concentrations from the rotating sites were adjusted for time trends by dividing TF for each respective week (Rivas et al., 2014). The rotating site concentrations were adjusted by using the following equation:

$$TF = \frac{(C^{Fixed\ site})_j}{(C^{Fixed\ site})}$$

$$(C_i^{Rotating\ site})^*_j = \frac{(C^{Rotating\ site})_j}{TF}$$

Where  $(C^{Fixed\ site})$  is the average NO<sub>2</sub> concentration at all fixed sites in the  $j$  measurement week,  $(C^{Fixed\ Site})$  is the mean annual concentration at all fixed sites,  $(C_i^{Rotating\ site})^*_j$  is the NO<sub>2</sub> concentration measure at the  $i$  rotating site in the corresponding  $j$  measurement week.

Seasonally adjusted rotating site concentrations were used to assess the spatial patterns of NO<sub>2</sub> in Holyoke, MA using land use characteristics while fixed-site data was used to examine the annual mean concentrations and seasonal trends. It is important to note that the results of this study were kept in micrograms per cubic meter (µg/m<sup>3</sup>) to allow for comparison with the WHO annual NO<sub>2</sub> guideline of 10 µg/m<sup>3</sup>.

To assess seasonal differences, specifically between Summer/Fall and Winter/Spring, we utilized R (Version 4.4.2; R Core Team, 2021) to perform a t-test comparing NO<sub>2</sub> mean concentrations across these periods. This analysis allowed us to determine whether there was a significant seasonal variation in the observed concentrations. Furthermore, to explore differences among site classifications—categorized as CHR, LD, and BG—we performed a one-way ANOVA using the “aov” function in R (R Core Team, 2021). This approach enabled us to assess whether NO<sub>2</sub> levels varied significantly based on site types, providing insights into the impact of land-use characteristics on air quality.

To evaluate how multiple predictors influence NO<sub>2</sub> concentrations in the city of Holyoke, we fitted a mixed effect model where NO<sub>2</sub> was added as a fixed effect and NO2\_ID and week\_year were added as random effects to account for differences across different locations, weeks, and

years (2021 and 2022). All numeric variables included in the model were standardized using the scale function in R.

### **1.2.6 Determinants of NO<sub>2</sub> concentration in Holyoke**

We employed standard regression model techniques, leveraging a spatially dense air pollution monitoring network and incorporating potential predictor variables typically derived from Geographic Information Systems (GIS) (Hoek et al., 2008). We reviewed findings from previous Land Use Regression (LUR) studies (Adamkiewicz et al., 2010; Mavko et al., 2008) to guide the selection of the predictor variables and buffer sizes around the measurement sites. We used 100 m, 200 m, and 300 m buffers as the most relevant for this project. This approach aimed to capture variations in dispersion patterns, scales of influence (local and background sources), and the geographical extent within Holyoke, MA. Using QGIS, we calculated the total length (in meters) of features such as road categories (interstates and secondary roads) and rivers/streams. We also estimated within each buffer the normalized difference vegetation index (NDVI). Additionally, we utilized the ‘worldmet’ R package (Carslaw, 2023) to retrieve meteorological data, including temperature, relative humidity, wind speed, and wind direction through the National Oceanic and Atmospheric Administration's (NOAA) Integrated Surface Database (ISD). All meteorological predictors were averaged weekly to align with the measurement data. Table 1 shows the candidate variables that were selected based on their spatial or temporal plausibility with the emission and dispersion of air pollution particularly NO<sub>2</sub>, in urban environments which was guided by the results of previous LUR models (Larkin et al., 2017; Cai et al., 2020; Cheewinsiriwat et al., 2016) and data availability.

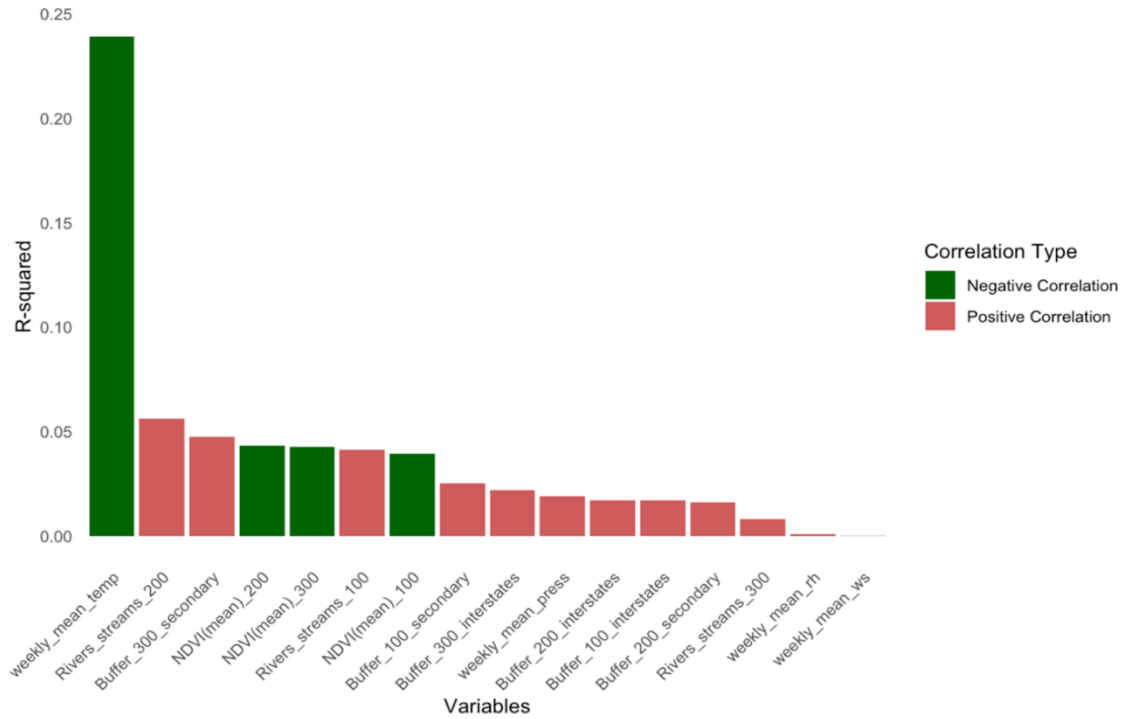
Table 1. Description of candidate spatial predictor variables

Variable (type)	Variable sub-categories	Source	Spatial statistics
Road network	a. Interstate and major roads b. Secondary roads	<a href="#">MassGIS tigger roads</a>	Sum of length of roads within buffer (m)
Land Use	a. Commercial/High-density residential b. Low-density residential c. background	Collected data	NA
Normalized Difference Vegetation Index (NDVI)	NA	<a href="#">United States Geological Survey - Landsat 8 imagery (30 m X 30 m)</a>	Average NDVI value within the buffer
Rivers and waterways	NA	<a href="#">MassGIS rivers and streams</a>	Sum of length of rivers and waterways (m)
Meteorological parameters	a. temperature b. relative humidity c. wind speed d. wind direction	Worldmet package R	Average weekly value
Months of the year	Seasons Time	Collected data	NA

Table shows all potential predictor variables used to build the models. The final models include a subset of these predictors chosen during the model selection process. Three circular buffer sizes with radii of 100 m, 200 m, and 500 m were considered. NA: not applicable.

We regressed the measured pollutant concentrations against site-specific geospatial predictors representing emission sources and dispersion patterns. First, we perform a Pearson’s correlation (r) matrix using the “cor” function in R to evaluate their associations with the measured NO<sub>2</sub> and among themselves. The strength of the association was used to identify variables most strongly associated with NO<sub>2</sub>. Figure 2 shows the magnitude of the association by squaring the r.

Figure 2. R-squared values



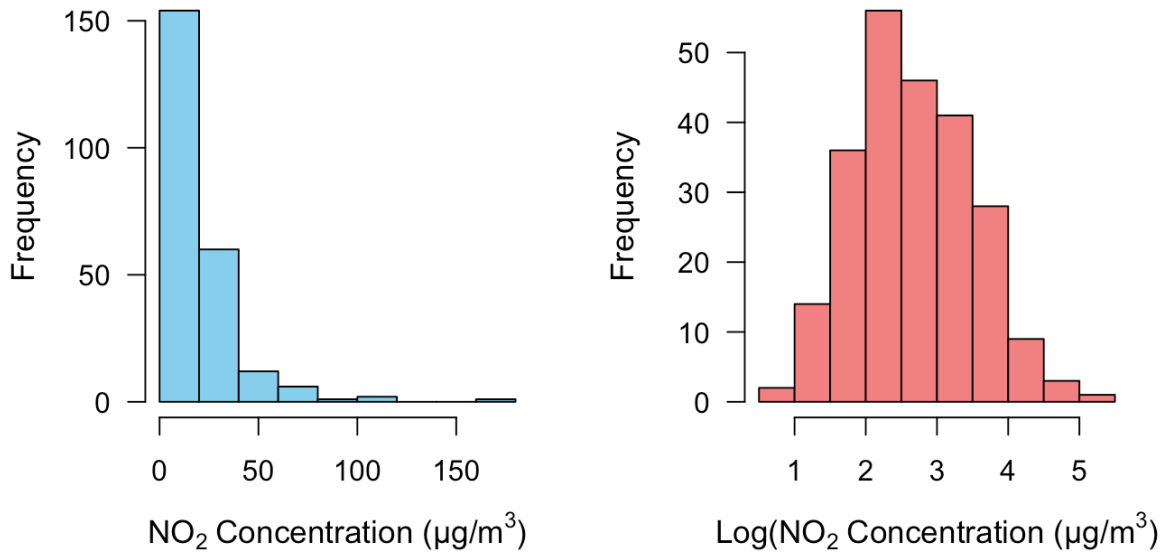
R-squared values show the proportion of variance in the response variable explained by each predictor variable. Positive correlations are indicated in red, while negative correlations are shown in green. Variables are ordered by their R-squared values, highlighting the relative strength of associations.

### 1.2.7 Model development

To ensure the appropriate development of our model, we assessed the distribution of our data to determine whether it followed a normal distribution or exhibited skewness. The NO<sub>2</sub> concentrations were found to be skewed. Consequently, we applied a log transformation to the data prior to conducting further analysis (Figure 3). We applied a forward stepwise regression procedure by systematically including in the model predictor variables with buffer radius that has the highest correlation with measured NO<sub>2</sub> concentrations. Selection of subsequent variables was made based on the magnitude of their added contribution to the model with a cut-off criterion of at least a 1% increase in adjusted R<sup>2</sup> and p-value < 0.05. Collinearity between variables was

assessed with a variable inflation detector (VIF) function from the R “car” package (Fox, 2019), and variables were excluded for  $VIF > 3$ . The process of variable selection continued until the inclusion of additional variables no longer improved the model.

Figure 3. Histogram of unlogged and logged nitrogen dioxide (NO<sub>2</sub>) concentrations

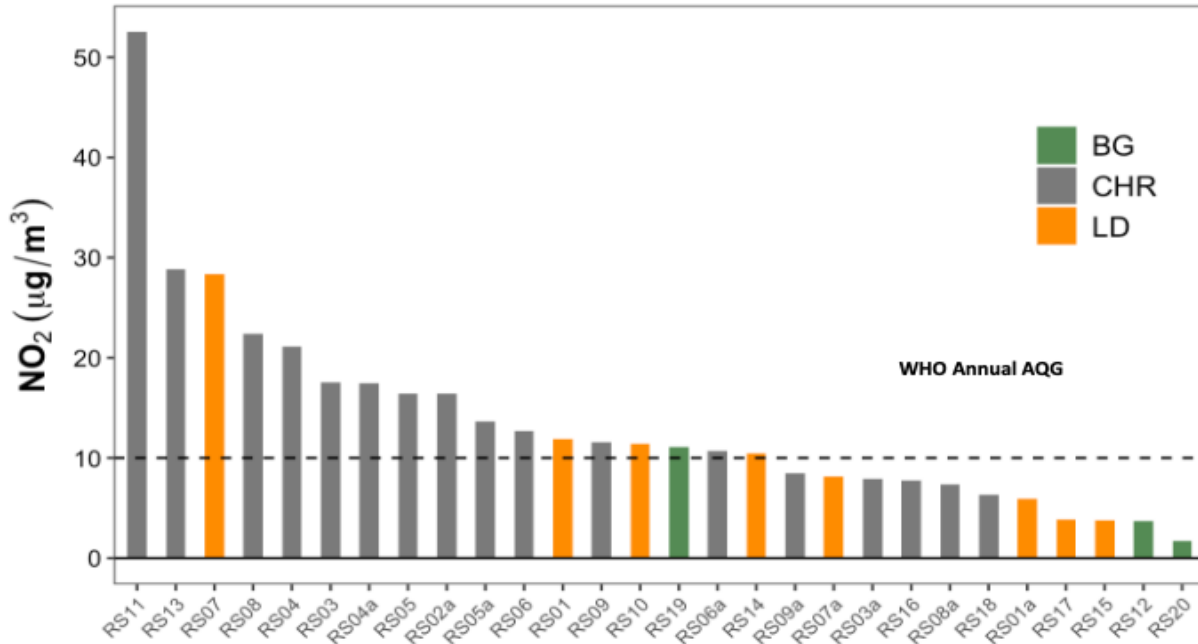


### 1.3.1 RESULTS

#### 1.3.2 Spatial patterns

We collected a total of 260 valid weekly samples from both fixed ( $n = 5$ ) and rotating ( $n=20$ ) sites during the one-year measurement campaign. The season-adjusted mean (SD) NO<sub>2</sub> concentrations across all the rotating sites was  $13.68 \mu\text{g}/\text{m}^3$  ( $10.18 \mu\text{g}/\text{m}^3$ ), with concentrations ranging from  $2.17 \mu\text{g}/\text{m}^3$  to  $55.14 \mu\text{g}/\text{m}^3$  (Table 2). Sites located in CHR areas experienced the highest mean concentration of  $17.09 \mu\text{g}/\text{m}^3$ , followed by LD areas ( $7.92 \mu\text{g}/\text{m}^3$ ) and the least at BG sites ( $5.50 \mu\text{g}/\text{m}^3$ ). Sites in the CHR tended to record some of the highest NO<sub>2</sub> concentrations (Figure 4). The annual equivalent at the rotating sites showed that NO<sub>2</sub> concentrations across Holyoke were meeting the US EPA standard of  $99.64 \mu\text{g}/\text{m}^3$ . However, nearly 61% of the sites exceeded the WHO guideline of  $10 \mu\text{g}/\text{m}^3$  (Figure 5.)

Figure 4. Seasonally adjusted weekly NO<sub>2</sub> concentrations for rotating sites



Bar plot shows the seasonally adjusted weekly NO<sub>2</sub> concentrations among each rotating site. The dashed line represents the current WHO Air Quality Guideline for NO<sub>2</sub>.

Table 2. Mean and standard deviation (SD) by site type

Site Type	Measurement (µg/m <sup>3</sup> )		
	Fixed	Rotating	All
<b>CHR</b>	25.89 (21.80)	17.09 (10.87)	24.25 (21.62)
<b>LD</b>	11.38 (10.55)	7.92 (3.45)	11.61 (10.43)
<b>BG</b>	13.56 (11.01)	5.50 (4.95)	13.71 (10.91)
<b>All Sites</b>	20.53 (19.75)	13.68 (10.18)	19.69 (18.95)

Table shows the mean and standard deviation in µg/m<sup>3</sup> across all site types and combined.

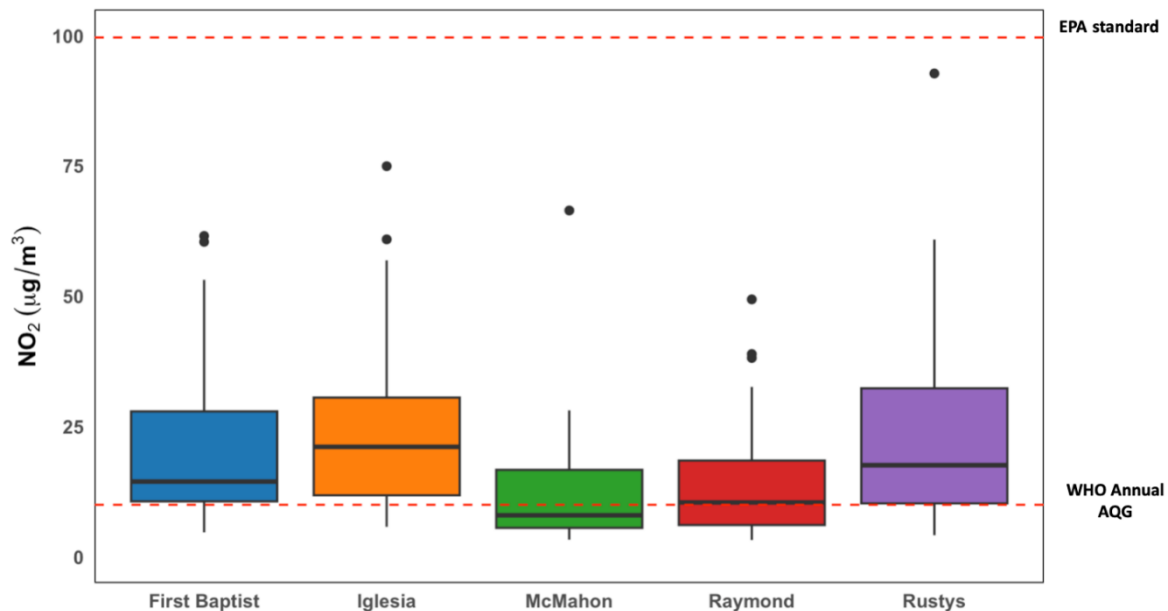
A one-way ANOVA comparing NO<sub>2</sub> concentrations by site type (CHR, LD, and BG) revealed a statistically significant difference in mean NO<sub>2</sub> concentrations across groups (F = 3.783, p = 0.0361). With p-value < 0.05, we can conclude that there is evidence that at least one site classification differs significantly from the other. Turkey's HSD Test of multiple comparisons found no statistically significant differences between LD-BG (0.9246) and CHR-

BG (0.1305). The difference between LD and CHR sites is marginally non-significant ( $p = > 0.05$ , but close to 0.05).

### 1.3.3 Temporal Patterns

The overall mean annual  $\text{NO}_2$  concentrations at the five fixed (year-long) sites were  $20.53 \mu\text{g}/\text{m}^3$  ( $19.75 \mu\text{g}/\text{m}^3$ ). Site-specific annual means ranged from  $12.28 \mu\text{g}/\text{m}^3$  to  $25.10 \mu\text{g}/\text{m}^3$ . Across the five fixed sites,  $\sim 1\%$  of the weekly samples exceeded the US EPA standard, and  $62\%$  exceeded the WHO guideline. Three sites saw over  $75\%$  of their weekly data surpassing the WHO guideline (Figure 6). Two of these sites also registered the highest levels above the US EPA standard ( $101.4 \mu\text{g}/\text{m}^3$  and  $163.7 \mu\text{g}/\text{m}^3$ ).

Figure 5. Box plot of the distribution of  $\text{NO}_2$  at the fixed sites

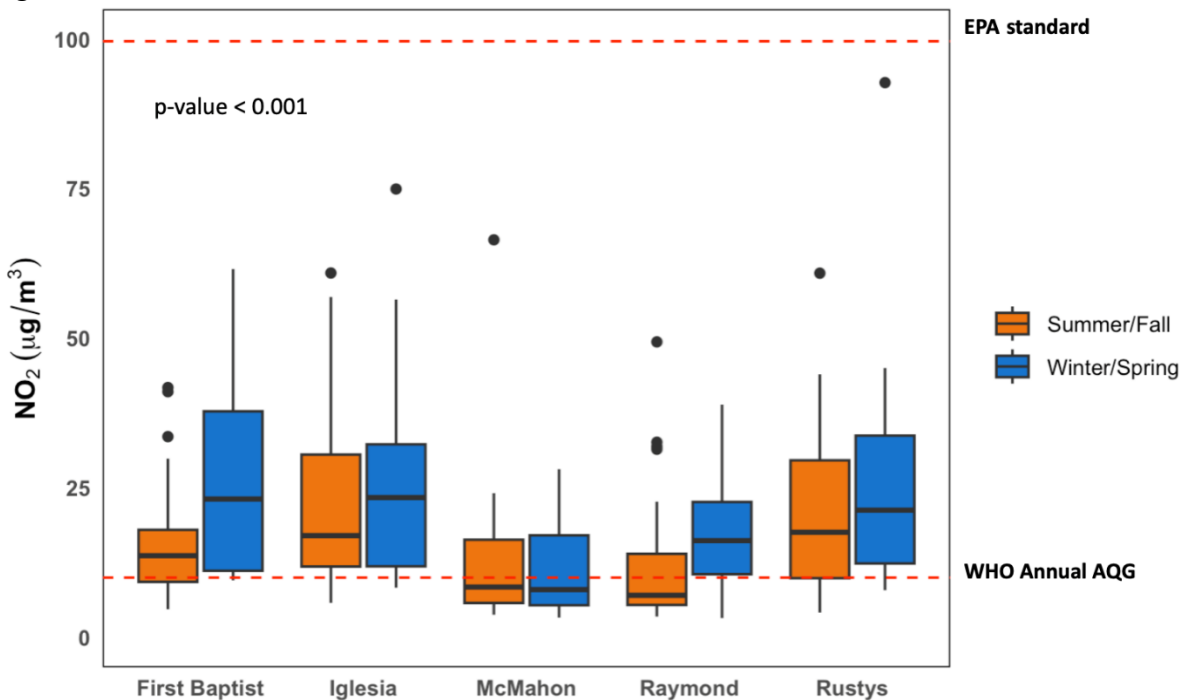


Box plot showing the distribution of  $\text{NO}_2$  concentration at the fixed (year-long) sites. Dotted red lines indicate the WHO air quality guidelines and EPA air quality standards.

### 1.3.4 Seasonal Patterns

Individual weekly NO<sub>2</sub> concentrations ranged from < 3.4 µg/m<sup>3</sup> in the summer to over 150 µg/m<sup>3</sup> in the winter. The winter seasonal mean NO<sub>2</sub> concentration of 47.8 µg/m<sup>3</sup> (28.5 µg/m<sup>3</sup>) was significantly higher than summer levels (47.8 vs 14.3 µg/m<sup>3</sup>, p = < 0.001) (Figure 7). There were 4 weeks in the winter where the levels exceeded the WHO guideline, compared to 17 weeks in the summer. Although there were only four weeks of exceedances during the winter, their exceptionally high levels significantly influenced and drove the majority of the observed results.

Figure 6. Seasonal variation of NO<sub>2</sub> concentrations at the fixed sites



Box plot shows the seasonal variation of NO<sub>2</sub> concentrations at the fixed (year-long) sites and statistical significance. Dotted red lines indicate the WHO air quality guidelines and EPA air quality standards.

### 1.3.5 Mixed Effect Model Results

The mixed effect model results showed that weekly average temperature, NDVI within a 200 m buffer, and weekly mean wind speed are key predictors influencing NO<sub>2</sub> concentrations. The variables explained ~51% of variations in the fixed effects components. The weekly average temperature has a strong negative association with NO<sub>2</sub> concentrations, with a slope estimate of -0.614 (95% CI: -0.753, -0.476). NDVI within a 200 m buffer also exhibits a negative relationship with NO<sub>2</sub> concentrations, with a slope estimate of -0.288 (95% CI: -0.414, -0.161), indicating that areas with greater vegetation density are associated with lower NO<sub>2</sub> levels. Similarly, weekly mean wind speed negatively impacts NO<sub>2</sub> levels, with a slope estimate of -0.174 (95% CI: -0.311, -0.038). In contrast, rivers within a 200m buffer and secondary roads within a 300m buffer do not significantly influence NO<sub>2</sub> concentrations, with slope estimates of -0.102 (95% CI: [-0.2475, 0.0436]) and 0.170 (95% CI: [-0.0133, 0.3523]), respectively. Overall, the findings highlight the importance of environmental factors such as temperature, vegetation, and wind speed in influencing NO<sub>2</sub> concentrations.

Table 3. Mean association of log NO<sub>2</sub> with spatial predictor variables in the final model

Predictors	Buffer sizes	Coefficient (95% CI)	Fixed effects R <sup>2</sup>
<b>Weekly mean temperature</b>	NA	- 0.614 (- 0.061, 0.199)	0.31
<b>Rivers and streams</b>	200	- 0.102 (- 0.753, -0.476)	0.38
<b>Secondary roads</b>	300	0.170 (- 0.248, 0.044)	0.40
<b>NDVI</b>	200	-0.288 (- 0.414, 0.161)	0.44
<b>Weekly mean wind speed</b>	NA	-0.174 (-0.311, -0.038)	0.51

Predictors of NO<sub>2</sub> concentration with slope coefficients, 95% confidence intervals, and cumulative R<sup>2</sup> for fixed effects. Buffer sizes indicate the spatial scale of analysis, while the cumulative R<sup>2</sup> reflects the proportion of variance explained by fixed effects in the mixed-effects model.

### 1.4.1 DISCUSSION

We conducted a city-wide year-long campaign to understand the spatial and temporal variations of NO<sub>2</sub> concentrations in Holyoke, MA, and to evaluate their potential determinants. We found that the city is meeting the US EPA annual standard for NO<sub>2</sub>. However, most areas in the city are exceeding the WHO's international health-based guidelines. Notably, commercial/high-density residential areas experienced the highest concentrations in comparison with low-density residential areas and background sites. NO<sub>2</sub> concentrations were also significantly higher during the winter/spring than in summer/fall, with the highest exceedances occurring in the winter. Temperature, green vegetation, and wind speed are explained as the most significant predictors of NO<sub>2</sub> concentrations in the city of Holyoke, collectively explaining ~51% of the model's variance.

Our findings of higher levels in high-density residential areas align with findings from previous studies (Stroshnider et al., 2017; Zhang et al., 2024), which also observed elevated NO<sub>2</sub> concentrations in high-density urban areas compared to rural zones. Findings are consistent with others that found higher NO<sub>2</sub> levels in urban areas and during winter seasons. For instance, studies in New Jersey found that the highest concentrations of NO<sub>2</sub> were experienced during the winter than in summer (Roberts-Semple et al., 2012; Foskinis et al., 2024). One of the potential explanations for this trend can be attributed to the seasonal planetary boundary layer height conditions and subsequent lower median wind speeds in fall and winter and a change in the diurnal wind pattern by season which can affect the dilution of air pollutants (Kendrick et al., 2015). In addition to the height of the boundary layer, temperature inversions can play a significant role in the concentrations of air pollutants. For example, when the boundary layer is lower, especially during inversions, it traps pollutants near the ground, while a higher boundary

disperses them more effectively (Zhanqing Li et al., 2017). Altogether, these patterns may explain some of the patterns observed during the study.

Other additional explanations may be related to the use of natural gas for heating during the winter (Ozgen et al., 2020) and the role of temperature on cold engine starts. Based on the US EPA, a cold start is defined as a start when the engine has been off for over 12 hours (US EPA, 2021a). The cold start phase of the gasoline direct injection is typically associated with less vaporized fuel spray and lean combustion, which can, in turn, generate more air pollutants, and the catalytic converter cannot be optimally efficient under low catalyst temperatures (Tu et al., 2020). Tu et al. (2020) observed that during the first trip of the day, after an overnight soak, the average  $\text{NO}_x$  was 384% and 299% higher than the emission rate on the second trip of the day.

The mixed effect model showed that temperature was inversely related to nitrogen dioxide ( $\text{NO}_2$ ). This may be explained by the photochemical reactions that occur in the presence of sunlight. When sunlight is abundant,  $\text{NO}_2$  reacts to form ozone ( $\text{O}_3$ ) through a series of processes. In this cycle,  $\text{NO}_2$  is broken down, and nitric oxide ( $\text{NO}$ ) is formed. This  $\text{NO}$  then reacts with free radicals generated by volatile organic compounds (VOCs) to regenerate  $\text{NO}_2$ , completing the cycle (Nguyen et al., 2022). During warmer temperatures, this process is more active, and much of the available  $\text{NO}_2$  is converted into ozone. As a result,  $\text{NO}_2$  concentrations decrease during the summer and spring months, while ozone levels rise. This seasonal dynamic is consistent with observed trends: higher  $\text{O}_3$  concentrations during warmer months and elevated  $\text{NO}_x$  ( $\text{NO} + \text{NO}_2$ ) levels during fall and winter, when cooler temperatures and reduced sunlight slow these photochemical reactions (Souza et al., 2024).

Our study also emphasized the significant role of wind speed in influencing NO<sub>2</sub> concentrations. Numerous land-use regression models have identified wind as a key predictor of NO<sub>2</sub> levels. Roman-Cascon et al. (2023) conducted a study comparing the relationships between wind and NO<sub>2</sub>, as well as turbulence and NO<sub>2</sub>, during winter and summer using sonic anemometers placed at two locations: one atop a building and the other near a roadway. Their findings revealed that turbulent variables correlated more strongly with pollutant concentrations at street level, while wind speed was a better predictor when measured from the terrace-level anemometer. Their analysis of turbulent diffusion behavior during winter showed that turbulence typically decreases during the evening transition, leading to the highest NO<sub>2</sub> concentrations. However, later at night, thermally driven winds often develop, which help disperse pollutants. These findings are consistent with our results, which demonstrate an inverse relationship between wind speed and NO<sub>2</sub> concentrations. They also underscore the importance of wind in mitigating air pollution, as stagnant conditions can lead to prolonged exposure to pollutants, especially in cities (Keshavarzian et al., 2022).

The study also demonstrated an inverse relationship between NDVI (Normalized Difference Vegetation Index) and NO<sub>2</sub> concentrations. Prathibha et al. (2023), as part of the Green Heart Louisville prospective cohort study, used Ogawa passive samplers to assess long-term, hyperlocal exposure to nitrogen oxides. Their research explored the connections between urban vegetation, local air quality, and cardiovascular health, revealing an inverse correlation between NO<sub>2</sub> levels and NDVI. This relationship is further supported by other studies, such as Larkin et al. (2017), which also found a negative association between NDVI and NO<sub>2</sub>. Areas with higher vegetation cover are often located in less disturbed, background sites, which tend to have fewer anthropogenic sources of pollution, thus contributing to lower NO<sub>2</sub> concentrations.

The mixed effect model showed no statistical significance between NO<sub>2</sub> concentrations and secondary roads. Typically, roadways tend to be highly influential (Larkin et al., 2017). However, roadways were not apparent in the model's prediction. Another study found a similar pattern when Terry et al. (2024) conducted a study using Ogawa passive samplers to monitor NO<sub>2</sub> concentrations at 15 sites in Philadelphia, Pennsylvania, USA, over two weeks during the fall, winter, and spring seasons. The predictor variables in their analysis included land use and land cover buffers, traffic counts, and distances to various types of roadways. Surprisingly, despite incorporating road-associated variables into the final model, the influence of roadways on NO<sub>2</sub> levels was not strongly evident, which aligns with our findings.

The motivation for this study stemmed from Holyoke's significant public health challenge with pediatric asthma cases (MACDC, 2023). One of our primary findings highlights that NO<sub>2</sub> concentrations in the area exceed the World Health Organization (WHO) air quality guidelines but remain within the U.S. Environmental Protection Agency (EPA) standards. This discrepancy highlights the need to examine health impacts even at levels below the EPA threshold. For example, in response to the WHO's revised annual mean NO<sub>2</sub> standard from 40 µg/m<sup>3</sup> to 10 µg/m<sup>3</sup>, Chen et al. (2024) conducted a meta-analysis of 11 studies published after the WHO's initial assessment. Their findings demonstrated a heightened risk of all-cause, cardiovascular, and respiratory mortality associated with long-term exposure to ambient NO<sub>2</sub>, with pooled risk ratios of 1.03 (95% CI: 1.02–1.05), 1.07 (95% CI: 1.04–1.10), and 1.03 (95% CI: 1.02–1.05) per 10 µg/m<sup>3</sup> increase in NO<sub>2</sub>. These results further emphasize the potential health risks posed by NO<sub>2</sub> exposure, even at concentrations below regulatory standards.

It is important to note that the number of high asthma cases in the city of Holyoke, MA might be influenced by other factors other than ambient NO<sub>2</sub> concentrations. For instance, the

number of asthma cases may be related to the air quality indoors rather than outdoors. For example, a study estimated NO<sub>2</sub> exposure and health consequences using emissions and concentration measurements from over 100 homes where the use of gas and propane stoves increased long-term NO<sub>2</sub> exposure by 4.0 parts per billion volume on average across the United States, 75% of the WHO's exposure guideline, where they indicate that this increased exposure likely causes approximately 50,000 cases of current pediatric asthma from long-term NO<sub>2</sub> exposure alone (Kashtan et al., 2024). Children living in urban neighborhoods often experience urban exposures that contribute to pediatric asthma morbidity, including exposure to pest allergens, mold, and endotoxins (Grant & Wood, 2022). They also experience disparities associated with the social determinants of health, such as increased poverty, poor housing quality, obesity, and chronic stress, which can exacerbate the complications associated with asthma (Grant & Wood, 2022). Further studies would benefit from incorporating data from multiple factors to understand the complexity of asthma, especially among marginalized communities.

#### **1.4.2 Strengths and Limitations of the Study**

One of the notable strengths of this study is its focus on a city predominantly composed of marginalized groups who are disproportionately burdened by respiratory disease. By examining NO<sub>2</sub> concentrations in Holyoke, MA, we contribute to understanding the environmental challenges faced by smaller, underserved urban areas. This research emphasizes the importance of stricter standards to protect vulnerable populations and highlights the relevance of studying air quality in smaller cities, which are often not studied.

One of the main limitations of this study is its geographic scope, which is restricted to Holyoke, MA, limiting the generalizability of the findings to other regions. It is also important to

note that our values represent weekly averages and do not account for daily variations. Additionally, the model did not include several potentially important predictors, such as meteorological variables (e.g., mixing layer depth, solar radiation, and water vapor mixing ratio), population density, or proximity to major and secondary roads (Wang et al., 2024). Future research should aim to address these gaps by incorporating these variables into the analysis. Furthermore, testing smaller buffer sizes, such as 50 meters, could be valuable, as previous studies have highlighted their significance when evaluating candidate variables (Babaan et al., 2024; Terry et al., 2024). Lastly, this study did not analyze nitric oxide (NO), which could provide additional insights into the dynamics of NO<sub>2</sub> concentrations and traffic-related sources (Carslaw, 2005). Future steps include collecting additional key predictor variables and assessing their influence using smaller buffer sizes. This approach will facilitate the development of a concentration surface map for unmeasured locations, based on the predicted concentrations for Holyoke, MA.

### **1.4.3 Conclusion**

In conclusion, our study shows the critical importance of understanding the spatiotemporal patterns of ambient NO<sub>2</sub> concentrations in urban areas, particularly those with large populations of vulnerable groups. These findings can significantly contribute to developing targeted strategies aimed at protecting communities most at risk. Furthermore, our analysis highlights the role of key variables such as NDVI, temperature, and wind in predicting NO<sub>2</sub> levels. By integrating these insights, our study advances the understanding of air pollution dynamics and provides a foundation for informed decision-making to mitigate environmental health risks in the city of Holyoke, MA.

## CHAPTER 2

### 2.1.1 INTRODUCTION

Climate change profoundly alters ecosystems, impacting plants and their interactions with pollinators (Trunschke et al., 2024). Heatwaves, or periods of two or more consecutive days of highly elevated day and night temperatures are becoming longer and more frequent around the world (Perkins-Kirkpatrick & Lewis, 2020). Heatwaves can influence plant traits, growth, and phenology, and can shape their interactions with arthropods (Mishra et al., 2023; Blaise et al., 2022). These changes in interactions can disrupt critical ecosystem services such as pollination, threatening natural biodiversity and agricultural productivity (Osman & Shebl., 2020). Understanding how these dynamics unfold is essential to predict and mitigate the cascading effects of climate change on biodiversity and ecosystem function.

Elevated temperatures significantly impact plant physiology, disrupting fundamental processes that underpin growth and productivity. High temperatures induce oxidative stress, increase water loss, and decrease overall plant growth (Hasanuzzaman et al., 2013). Heat stress can also disrupt dry matter partitioning and photosynthesis, reducing the efficiency of energy capture and assimilation. The physiological impacts can include damage to the photosynthetic apparatus and impaired metabolic functions, limiting plant vigor and development (Bita & Gerats, 2013). Elevated temperatures also decrease the net assimilation rate, a key measure of how plants convert absorbed energy into biomass, thereby hindering growth and productivity (Vernon et al., 1963). These physiological disruptions show the susceptibility of plants to rising temperatures and how heat exposure can reduce future plant productivity in a warming climate.

The effects of extreme heat extend to developmental processes, particularly flowering and reproduction. Heat stress caused by temperature fluctuations can alter protein structures,

delaying key developmental stages, such as flowering initiation, and reducing reproductive success (Tun et al., 2021). Extreme heat further exacerbates these issues by reducing the net photosynthesis rate and decreasing non-structural carbohydrate concentrations in leaves, which are vital for energy storage and plant development. This physiological imbalance results in fewer flowers, lower yields, and reduced fruit sets unless plants are supplemented with additional water (Borghini et al., 2019). These temperature-induced physiological disruptions highlight the heightened vulnerability of plants during critical growth and reproductive phases. Understanding how rising temperatures impact plant physiology, floral traits, and phenology is essential for developing adaptive strategies to mitigate these effects. From safeguarding metabolic processes to enhancing water use efficiency, addressing these challenges is critical for ensuring plant health, development, and productivity in the face of increasingly extreme climate conditions.

Beyond affecting plant traits, climate change can also disrupt plant phenology—the timing of life-cycle events—by delaying or accelerating blooming in various plant species (Craufurd and Wheeler, 2009). This shift in the timing of blooming can indirectly influence pollinator behavior by altering plant attractiveness, potentially leading to reduced pollination success (Descamps et al., 2021). Flower visitation is closely tied to insect abundance and the synchronization between the insects' flight periods and the plant's blooming phase (Fisogni et al. 2015). For instance, Rafferty & Ives (2010) showed that for plants that usually bloom at the same time each year, an earlier shift in phenology resulted in a decrease in floral visitors. In addition to plant phenology, extreme temperature exposure to plants during early bloom can also alter pollinator behavior. For example, in a similar study, Walters et al. (2024) demonstrated that heat stress exposure during early bloom significantly reduces the attractiveness of plants to pollinators, with female blue orchard bees (*Osmia lignaria*) laying 70% fewer eggs on heat-

stressed blueberry (*Vaccinium corymbosum*). These findings highlight the potential for climate change, particularly elevated temperatures, to disrupt plant-pollinator interactions, reduce pollination efficiency, and threaten both biodiversity and agricultural productivity.

Climate change poses significant threats to plant-pollinator interactions, influencing crop production and biodiversity (Vasiliev et al., 2021; Prather et al., 2012). Pollinator-dependent crops play a critical role in nutrition as they provide key vitamins, minerals, and antioxidants (Eilers et al., 2024). The absence of animal pollination could reduce total agricultural production by 3% to 8% (Aizen et al. 2009), underscoring the vital role of pollinators in maintaining food systems. These challenges are further exacerbated in low-income areas, where urban heat islands, limited green spaces, and environmental inequities place additional strain on pollinator habitats and crop production efforts (Pandey & Gosh, 2023).

Fruits and vegetables, such as tomatoes, can play a key role in providing nutrition for community members in low-income areas, being a staple in community gardens and urban farms due to their fast growth, high nutrient content, and gastronomical versatility (Richardson & Arlotta, 2022). Moreover, tomatoes account for a high proportion of human fruit consumption in many parts of the world (Wang et al., 2023), and their yields can be improved through biotic pollination (Bashir et al., 2017). However, in tomatoes, increased temperatures of 5°C have experimentally been shown to reduce the duration of fruit growth by five days and decrease the accumulation rates of fresh and dry matter (Ruiz-Nieves et al. 2020). Any negative impact on their cultivation could have significant consequences. The reduction in the duration of fruit growth and accumulation rates of fresh and dry matter show the vulnerability of tomato production to climate warming, emphasizing the need for strategies to sustain crop yields and quality in a changing climate. The effects of extreme temperatures are especially pronounced in

human-modified landscapes, such as urban environments, where the effects of heatwaves are intensified through the heat island effects (Moriarty & Honnery et al., 2014).

Given the potential climate change-driven physiological impacts on plants and the disruptions of plant-pollinator interactions in tomato production systems, we experimentally evaluated the role of heatwaves on plant traits and indirect consequences for pollinator attraction using tomatoes grown in urban areas. The study area was primarily community gardens, as they can harbor diverse pollinator groups (Neumann et al., 2024). We evaluated whether plant exposure to simulated heatwave conditions influenced plant growth (final height and growth rate), flowering (number of flowers and phenology), and fruit development (number of immature and mature fruit and phenology). We assessed whether heatwave exposure impacted the abundance and diversity of floral and non-floral visitors to the plants. We predicted that heatwave exposure would reduce plant growth, and delay flowering and fruit phenology, ultimately reducing the number of mature fruits developed. Furthermore, we predicted that heatwave exposure would decrease the number of floral visitors and increase the number of non-floral visitors. Understanding how climate change, particularly heatwaves, impacts plant health and pollination is crucial for developing strategies to mitigate these stresses, especially in vulnerable low-income urban environments. Our study will provide valuable insights into these dynamics, which will help in the design of effective strategies to address these challenges.

## **2.2.1 METHODS**

### **2.2.2 Plant Model**

The plant model for this project was cherry tomato (*Solanum lycopersicum var. cerasiforme*, variety ‘super sweet 100’), selected because it is often grown in community gardens and urban areas (Richardson & Arlotta, 2022). *Solanum* plant species, such as cherry tomatoes, rely on

buzz pollination—a process in which bees use vibrations to release pollen from flowers with specialized morphologies (Cooley & Vallejo-Marin, 2021). Plant plugs were purchased from Western Growers Inc. (~15 cm tall; n = 96). Each plant was given a unique identification number and transferred to two plant growth chambers (model 73-1122, Caron). The plants remained in the chambers for four days (June 3<sup>rd</sup>, 2024, to June 6<sup>th</sup>, 2024) under standard conditions of 28.9° C from 6:00 AM-6:00 PM and 23.9 ° C from 6:01 PM-5:59 AM (temperature selected based on NOAA’s National Weather Service, n.d.) and watered daily to ensure all plants had approximately equal moisture. After the four days, the plants were either exposed to heatwave or control conditions.

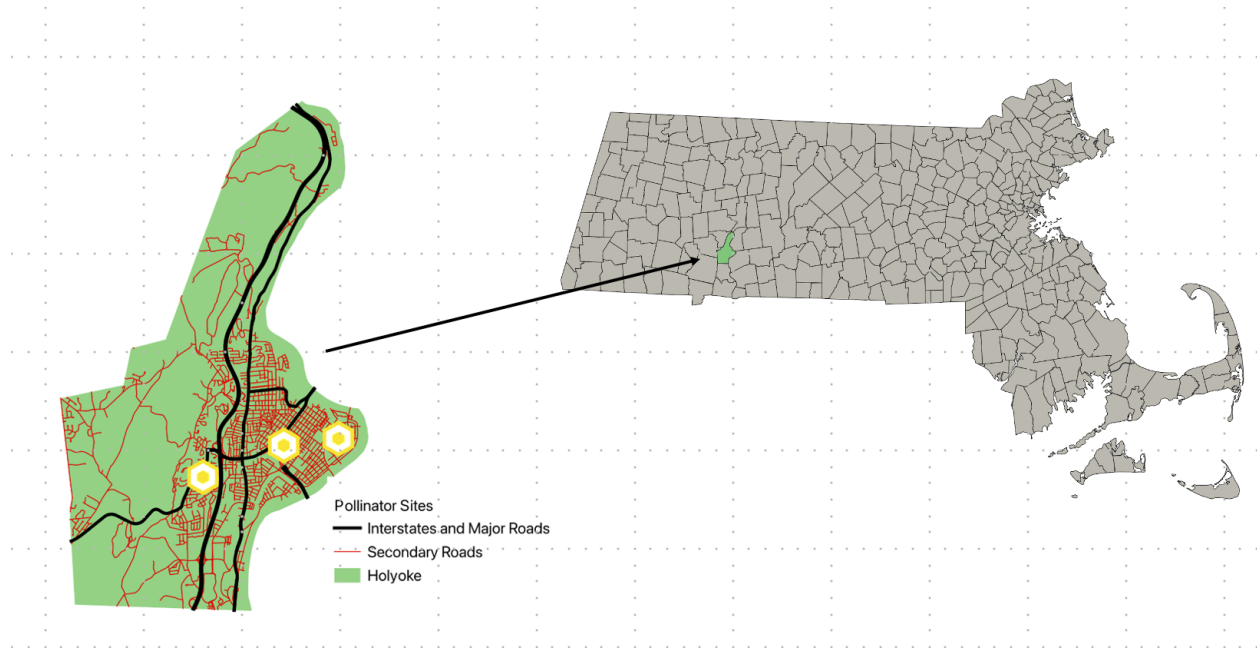
### **2.2.3 Experimental Heatwave Exposure**

A key feature of heatwaves is a reduction in variation between daytime and nighttime temperature (Habeeb et al., 2015), being defined as a period of two or more consecutive days where the daily minimum apparent temperature is higher than the 85th percentile of historical temperatures for the area (USGCRP et al., 2017). As such, the plants were randomly placed into two treatments: a heatwave treatment group (HW) (n = 45) exposed to a constant 37.8° C for three consecutive days (*Extreme Heat Safety Tips*, n.d.), and a control group (C) (n = 45) exposed to 28.9° C from 6:00 AM-6:00 PM and 23.9 degrees Celsius from 6:01 PM-5:59 AM from June 7<sup>th</sup>, 2024 to June 10<sup>th</sup>, 2024 (temperatures were selected based on records from NOAA’s National Weather Service that were geographically relevant for the city of Holyoke, MA). We acknowledge that this experimental design does not include the fluctuation in day and nighttime temperatures; the temperatures were selected as extreme conditions and would benefit from complementary studies that include a range in daily maximum and range of temperature fluctuation. After completing the exposure treatments, the plants were transplanted into 3.5-

gallon pots filled with a loam and compost mixture sourced from Martin’s Farm Compost and Mulch.

#### 2.2.4 Site Selection and Field Season Duration

Figure 7. Sampling sites



Map of Holyoke, MA with yellow figures indicating the sites chosen for the study (La Piedra Garden, Youth Garden, and Holyoke Community College). This map also shows interstates, major roads, and secondary roads and the city’s location within the state of Massachusetts.

The plants were established at three sites in the city of Holyoke in Massachusetts: two community gardens (Youth Garden and La Piedra Garden) and the greenspace of a community college (Holyoke Community College, HCC) (Figure 1). We selected sites with a similar proportion of developed land in a 1-mile radius around the site (calculated using Beescape: average = 76%, range = 59% - 77%; Prestby et al., 2022). Plants were deployed June 11<sup>th</sup>, 2024, and monitored until August 22<sup>nd</sup>, 2024. It is important to note that 7 days after deployment in the field, a naturally occurring heatwave took place on June 18<sup>th</sup> through June 20<sup>th</sup>, 2024, with temperatures reaching up to 105°F or 40.55°C (Cote, 2024), and thus half of the plants were

exposed to two consecutive heatwaves (one experimental and one naturally occurring) while the other half was exposed to one (naturally occurring).

At one of the sites (Youth Garden), the HW plants were placed in an area of the garden later discovered to have highly fertile potting soil, while the C plants at that site were placed in standard soil (grass), which resulted in the HW plants rooting through their pots and having access to more nutrients than the C. At the other two sites, both the HW and C plants were all placed on standard soil (grass). Thus, the data are analyzed for all sites combined as well as for La Piedra and Holyoke Community college separately, removing Youth Garden, given the potential impact of additional nutrient access.

### **2.2.5 Plant Growth and Phenology Surveys**

Sites were watered and surveyed weekly, with the following data collected: the height of each tomato plant was measured once per week (weekly survey), while the number of flowers and immature/mature fruits was recorded three times per week (daily survey). Plant height was measured in centimeters (cm) using a measuring tape (the tallest branch of each plant was straightened and measured). Weekly height measurements began on the deployment date (June 11th, 2024) and continued throughout the study period. To investigate plant growth, we calculated growth rates over the first two weeks post-experimental warming as an initial assessment of plant growth (June 17, 2024, to July 2, 2024). We calculated the initial growth rate for each plant as the proportional change in height between these two-time points ( $(\text{final} - \text{initial})/\text{initial}$ ).

During each daily survey, the number of flowers open at the time of observation was recorded. Fruits were classified as follows: mature fruits exhibited full maturation signs, such as a deep red color and softness to the touch, while immature fruits were green, firm, and typically

smaller in size. Plants were watered until the soil was moist, as needed. To evaluate the timing of key phenological events in plants, we analyzed flowering and fruiting phenology across different sampling rounds. For each plant, we calculated the earliest sampling round when flowers were observed (first bloom round) and the earliest round when mature fruits appeared (first mature fruit round). These metrics allowed us to quantify phenological timing at an individual level.

### **2.2.6 Floral and Non-floral Visitor Surveys**

Each site was surveyed three times per week (the order in which the sites were visited was randomized). During each survey, we recorded temperature, wind, cloud cover, and treatment. Temperature was obtained from the Weather Channel app, using the recorded temperature for the city at the time of the survey. Wind conditions were assessed visually and categorized as still, light breeze, or windy. Cloud cover was estimated based on the amount of light reaching the focal patch, and categorized as full sun, partial shade, or full shade.

We conducted visual surveys of the floral visitor communities visiting the tomato plants. Plants from each treatment group (control and heatwave) were monitored for 15 minutes. We tallied the number of visitors that made contact with the reproductive parts of the flowers. The visitor taxa were classified as: bumble bees (*Bombus* spp.), honey bees (*Apis mellifera*), carpenter bees (*Xylocopa virginica*), sweat bees (Halictidae, primarily Augochlorini), syrphid flies (Syrphidae), butterflies and moths (Lepidoptera), and “other”. The “other” category included all floral visitors touching the reproductive parts of the plants, including wasps and other insects that the team was unable to clearly identify in the field.

Non-floral visitors present on the plants were assessed for each plant once per week. Insects touching the reproductive parts of the flower during the survey were not counted. The taxonomic resolution of this survey was to the Order level, including spiders (Araneae), beetles

(Coleoptera), flies (Diptera), true bugs (Hemiptera), moths and butterflies (Lepidoptera), and “others”. The “other” category included insects not belonging to the insect orders listed above and insects that we were unable to identify. This assessment was conducted categorically from June 17<sup>th</sup>, 2024, to July 18<sup>th</sup>, 2024 (A = 0 individuals, B = 1-10, C = 11-20, D = 21+). We observed that most of the plants did not exceed the “A” category (70% of observations) and thus after July 18<sup>th</sup> recorded the exact number of insects present for the remainder of the season instead of as a category. Floral and non-floral visitor surveys were not conducted on days with high winds or extensive cloud cover. Windy conditions were defined as days when leaf movement was substantial enough to interfere with observations, while high cloud cover referred to overcast days with minimal direct sunlight on the focal patch.

### **2.2.7 Surrounding Plant Species Richness**

Using iNaturalist (iNaturalist, 2008), we recorded the presence of plants surrounding the focal patch once a week. With the data collected, we calculated the surrounding plant species richness. This was done by grouping the data by site and date and counting the number of unique plant species observed in each grouping.

## **2.3.1 STATISTICAL ANALYSIS**

### **2.3.2 Applications, Software, and Packages**

All analyses were performed using R (Version 4.4.2; R Core Team, 2021) using generalized linear mixed models (GLMM) using either the R package ‘lme4’ (Bates et al., 2015) or glmmTB (Brooks et al., 2017) to determine the effects of temperature on floral visitors, plant growth, flowering, and fruit development. We evaluated the effect of the heatwave treatment on the initial plant growth rate, weekly plant height measurement, initial number of flowers produced (during the first two sampling dates in which height was recorded ), total number of

flowers produced, flower phenology (time when flowers first observed), total number of fruit (immature and mature fruit), and fruit phenology (time when fruit first observed). To evaluate the total number of immature fruits and non-floral visitor abundance, zero-inflated models were fitted. Models varied in whether they were analyzed at an individual plant level (n = 96 total plants equally divided by the two treatments), a daily observation level (n = 288, 3 days of sampling per week), or a weekly observation level (n = 761, dates when height was measured). We included site as a random effect in all models, and the unique ID of each plant and sampling date as additional random effects for the weekly observation level analyses (Table 1). Significance was determined using the Anova function of the ‘car’ package (Weisberg, 2019). Model assumptions were verified using the R package ‘DHARMA’ before modeling to ensure proper fit (Hartig, 2024). After evaluating each model's assumptions, we found that the total number of flowers, immature fruits, and fruit phenology models violated the Levene test for homogeneity of variance. Despite this limitation, the models performed well in meeting all other assumptions. Lastly, to assess the differences among floral visitors, we used the ‘emmeans’ package (Lenth, 2024) and ‘dplyr’ (Wickham et al., 2023) packages to analyze and visualize the differences between groups.

Table 4. Plant model summaries

<b>Response</b>	<b>Model</b>	<b>Unit of replication</b>	<b>Distribution and link function</b>
1. Initial growth rate in the field (log transformed)	initial growth rate ~ heatwave (heatwave vs control[treatment]) + (1 site])  Factors: heatwave (control vs heatwave), site_name	Individual plant level (n = 96, equally divided among both treatments)	Gaussian distribution Link = Identity

	Numeric: Growth rate defined as height (2 weeks post heatwave exposure) – initial height (immediately after the heatwave exposure) / initial height		
2. Weekly measurement of plant height (cm)	Height of tomato plants[height_cm] ~ heatwave (heatwave vs control[treatment]) + (1 site_name) + (1 individual plant measurements[unique_id]) + (1 date)  Factors: treatment, site name and date  Numeric: height and unique_id (plant ID)	Weekly observation (n = 761, 96 plants measured once a week for 8 weeks)	Gaussian distribution Link = Identity
3. Initial number of flowers	Number of flowers by the end of the first week [n_flowers] ~ heatwave (heatwave vs control[treatment]) + (1 site_name)  Factors: treatment and site_name  Numeric: number of flowers by the end of the second week	Daily observation level (n = 288), 96 plants measured during the first 3 days of sampling	Poisson distribution Link = log
4. Total number of flowers	Total number of flowers ~ heatwave (heatwave vs control[treatment]) + (1 site_name)  Factors: treatment, site name  Numeric: total number of flowers	Individual plant level (n = 96, equally divided among both treatments)	Negative binomial distribution Link = log
5. Flower phenology (time when flowers first observed)	Flower phenology (sampling round [numeric] of first bloom) ~ heatwave	Individual plant level (n = 96, equally	Poisson distribution Link = log

	<p>(heatwave vs control[treatment]) + (1 site_name)</p> <p>Factors: treatment and site name</p> <p>Numeric: sampling round</p>	divided among both treatments)	
6. Fruit phenology (time when fruit first observed)	<p>Fruit phenology (sampling round [numeric] of when plant produce fruit for the first time) ~ heatwave (heatwave vs control) + (1 site)</p> <p>Factors: treatment and site name</p> <p>Numeric: sampling round</p>	Individual plant level (n = 96, equally divided among both treatments)	Negative binomial model Link = nbinom2
7. Total number of immature fruits	<p>Immature_fruit ~ heatwave (heatwave vs control[treatment]) + (1 site)</p> <p>Factors: treatment, site name and date</p> <p>Numeric: number of immature fruits</p>	Individual plant level (n = 96, equally divided among both treatments)	Negative binomial distribution Link = nbinom2
8. Fruit phenology (time when fruit first observed)	<p>Fruit phenology (sampling round [numeric] of when plant produce fruit for the first time) ~ heatwave (heatwave vs control) + (1 site)</p> <p>Factors: treatment and site name</p> <p>Numeric: sampling round</p>	Individual plant level (n = 96, equally divided among both treatments)	Negative binomial model Link = nbinom2

Table 5. Floral and non-floral visitor models summary

<b>Response</b>	<b>Model</b>	<b>Link function</b>
9. Abundance of floral-visitor	<p>abundance of floral visitors ~ heatwave (heatwave vs control [treatment]) + plant richness + (species_group) + (1   site_name) + (1   date)</p> <p>Factors: heatwave (control vs heatwave), species_group, site_name and date</p> <p>Numeric: abundance of floral visitors and plant richness</p>	<p>Negative binomial distribution</p> <p>Link = nbinom2</p>
10. Abundance of non-floral visitor	<p>abundance of non-floral visitors ~ heatwave (heatwave vs control [treatment]) + plant richness + (herbivore_groups) + (1   site_name) + (1   date)</p> <p>Factors: heatwave (control vs heatwave), herbivore_groups, site_name and date</p> <p>Numeric: abundance of non-floral visitors and plant richness</p>	<p>Poisson distribution</p> <p>Link = log</p>

### 2.3.3 Statistical analysis applied to models

To evaluate the effects of treatment on initial growth rate, flower and fruit phenology, and the total number of mature and immature fruits and flowers, we used a generalized linear mixed model (GLMM) with individual plants as the unit of replication. Treatment was included as a fixed effect, and sites were modeled as a random effect. Initial growth rate was modeled using a Gaussian distribution with an identity link function, while the flower phenology model and total number of mature fruits model were fitted using a Poisson distribution with a log link

function. In contrast, the fruit phenology model and the total number of immature fruits models were fitted using a negative binomial distribution with a `nbinom2` link function.

Weekly measurements of plant height (cm) were modeled with treatment as a fixed effect and sites, individual plants, and dates as random effects, following a normal distribution with an identity link function. The initial number of flowers was modeled using a Poisson distribution with a log link function. The abundance of floral and non-floral visitors was modeled using multiple fixed effects, including treatment, plant richness, morphological groups, and non-floral visitor groups. The models included site and date as random effects. The abundance of floral visitors was analyzed using a negative binomial distribution with a `nbinom2` link function, whereas the non-floral visitor model was analyzed using a Poisson distribution with a log link function. This approach allowed us to capture the variation in plant and visitor responses across treatments and sites while accounting for additional sources of random variation where appropriate.

### **2.3.4 Statistical Evaluation of Models Excluding Youth Garden**

We wanted to understand the influence and effect of the confounding factor associated with the youth garden (additional exposure to nutrients in the HW treatment compared to the C). We re-analyzed all of the variables excluding data from this site and reported statistically significant differences in the main results and all results in supplementary text.

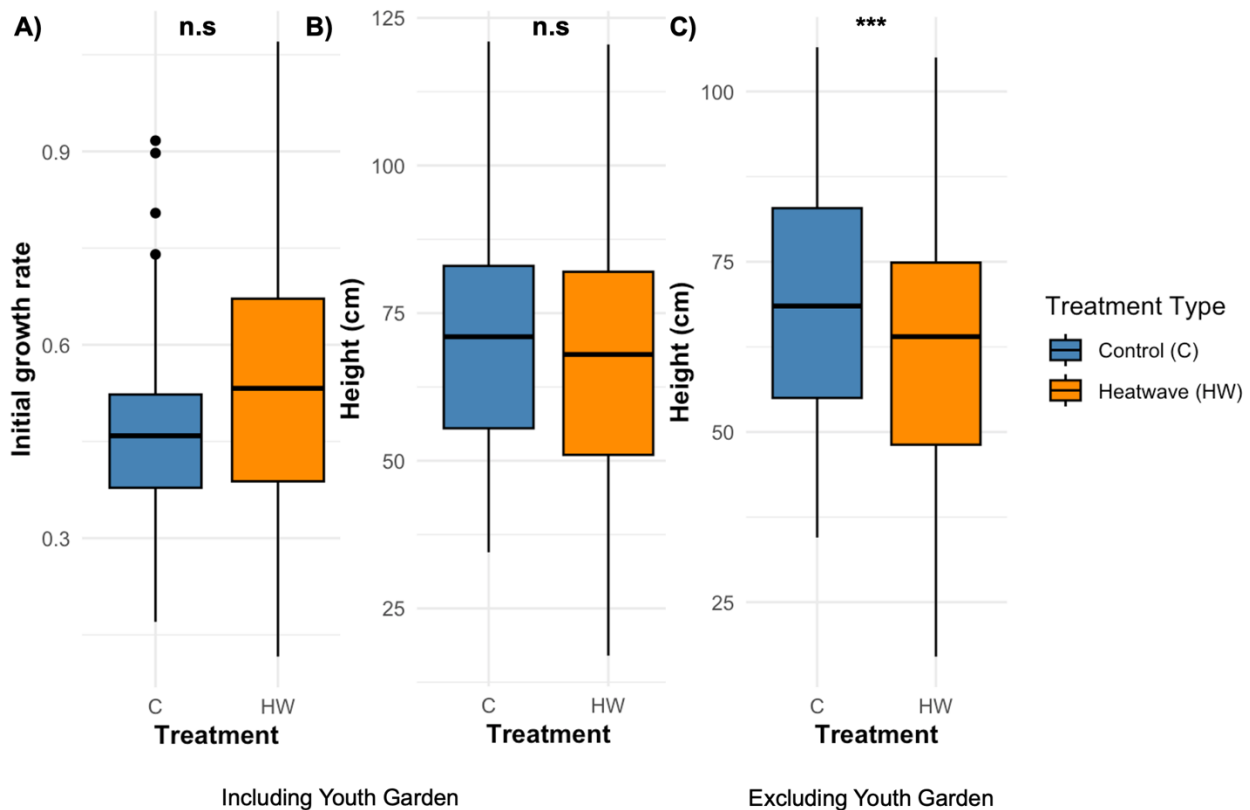
### **2.4.1 RESULTS**

#### **2.4.2 Plant Growth**

Initial heatwave exposure did not significantly influence initial plant growth rate ( $\chi^2 = 0.30$ ,  $df = 1$ ,  $p = 0.58$  (Figure 8A)). There was no significant effect on the weekly plant height ( $\chi^2$

= 2.53, df = 1, p = 0.11) (Figure 8B). However, when youth garden was excluded, we found a statistically significant effect between treatments ( $\chi^2 = 17.65$ , df = 1, p = < 0.001), where HW exposure resulted in a *decrease* in a weekly plant height of approximately 5.95 cm compared to the control (Figure 8D).

Figure 8. Box plot of plant growth and height



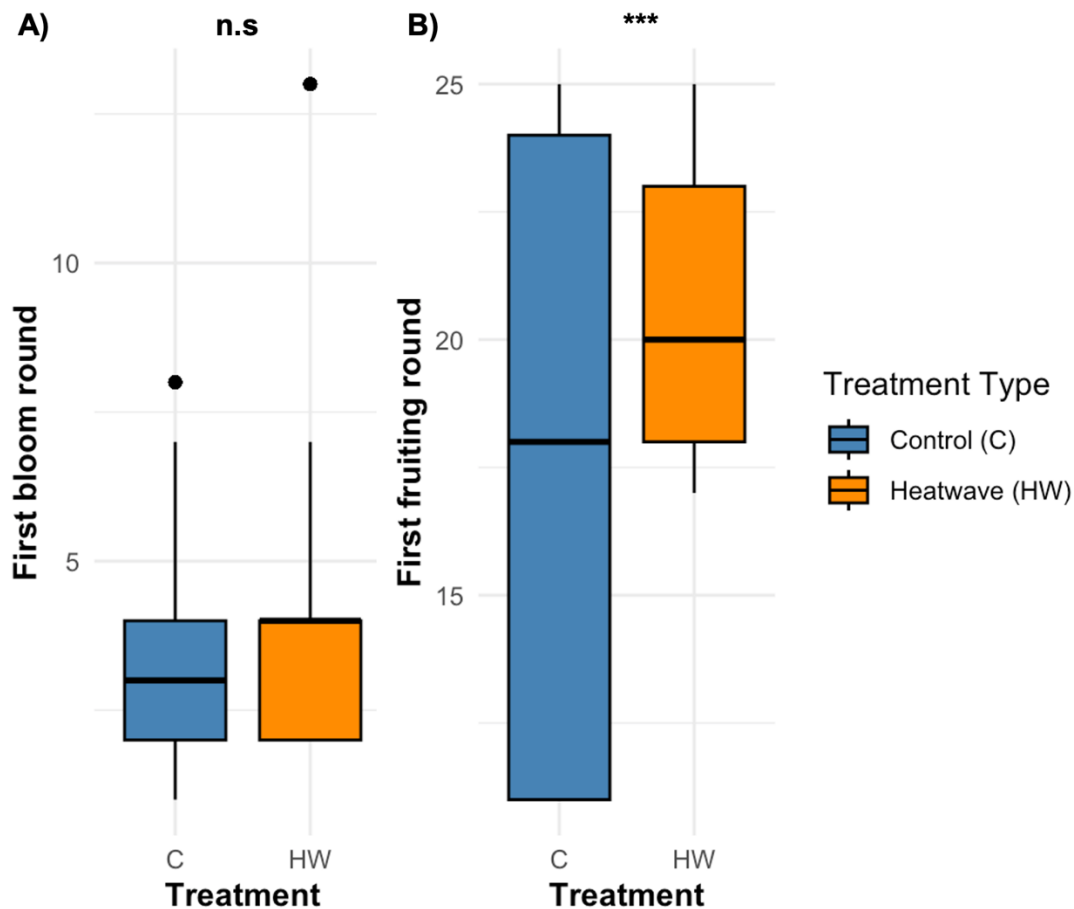
Box plots of plant growth and height including and excluding Youth Garden, the site with additional access to nutrients. A) Initial growth rate calculated from the first week after deployment to the field. B) weekly height measurement in cm of tomato plants between treatments. C) weekly height measurements in cm of tomato plants between treatments excluding Youth Garden. To indicate statistical significance, we used (n.s) for non-significant results and (\*\*\*, p < 0.001) for significant results.

### 2.4.3 Flower and Fruit Phenology

The heatwave exposure did not significantly affect flower phenology, as indicated by the timing of the first bloom ( $\chi^2 = 0.231$ , df = 1, p = 0.630) (Figure 9A). In contrast, the fruit phenology model revealed a statistically significant shift in fruiting patterns under heatwave

treatment compared to the control ( $\chi^2 = 5.23$ ,  $df = 1$ ,  $p = 0.022$ ). The positive effect estimate ( $\beta = 0.112$ ) suggests that the experimental heatwave delayed the fruiting period relative to the control group (Figure 9B). Notably, this pattern persisted even after excluding the youth garden site ( $\chi^2 = 110.5$ ,  $df = 1$ ,  $p < 0.001$ ).

Figure 9. Plant and fruit phenology box plots

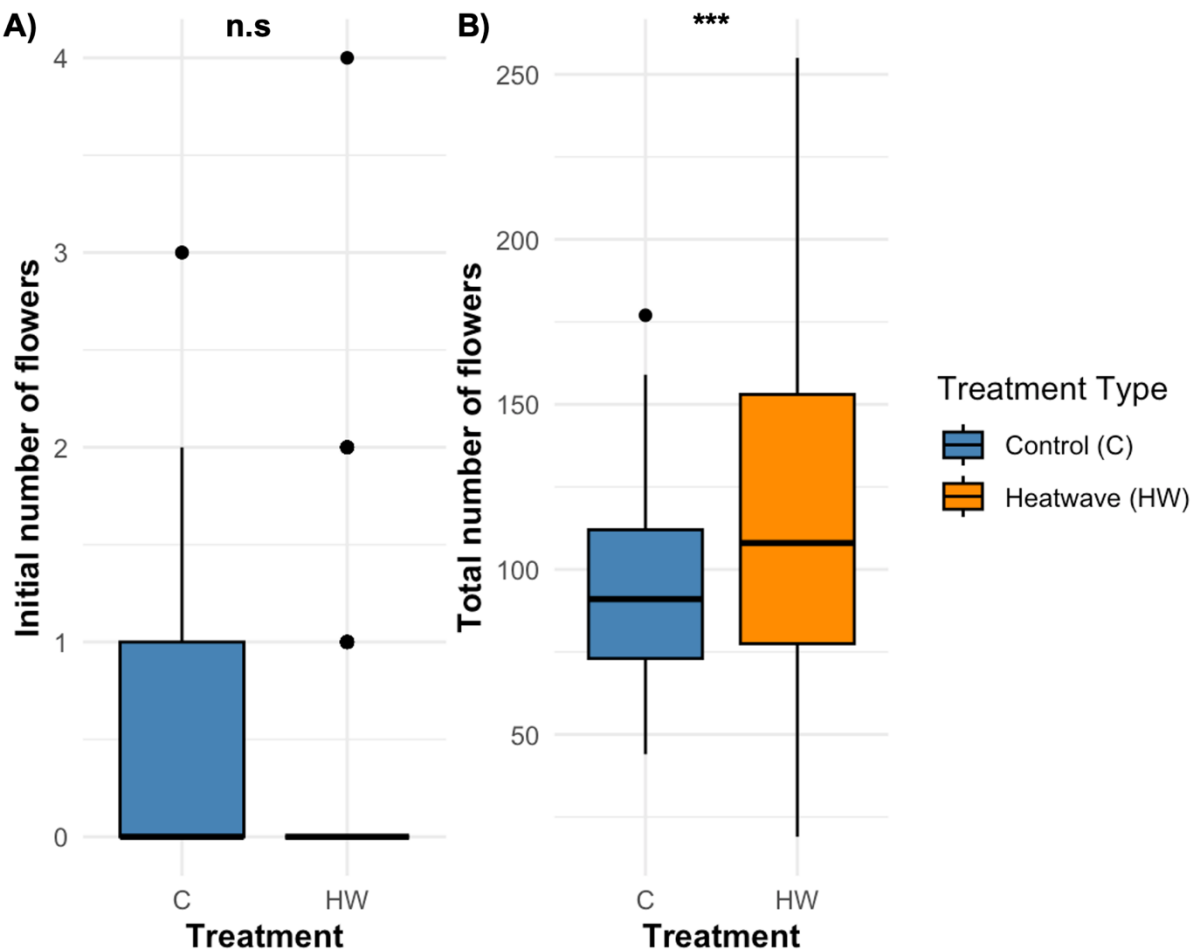


Box plots of plant and fruit phenology. A) the phenology of tomato plants, specifically the timing of the first flowering and fruiting events, under heatwave (HW) and control (C) treatments. The first flowering round represents the earliest sampling round when flowers were observed, while the first mature fruit round indicates (B) the earliest period when mature fruits were recorded, under heatwave (HW) and control (C) treatments. To indicate statistical significance, we used (n.s) for non-significant results and (\*\*\*,  $p < 0.001$ ) for significant results.

#### 2.4.4 Flower Count

The heatwave treatment (HW) had no significant impact on the number of flowers in bloom by the end of the first week (Figure 10A). The estimated effect size was minimal (-0.019 on the log scale), with no evidence to support a difference in flower counts between heatwave and control conditions ( $\chi^2 = 0.0098$ ,  $df = 1$ ,  $p = 0.921$ ). In contrast, the heatwave treatment significantly increased the total flower counts (estimate = 0.19,  $\chi^2 = 11.15$ ,  $df = 1$ ,  $p < 0.001$ ), with heatwave-exposed plants producing 22% more flowers compared to controls (Figure 10B).

Figure 10. Box plot of number of flowers



Box plots of number of flowers. A) Initial number of flowers observed during the first week of sampling under two treatments: heatwave (HW) or Control (C). B) Total number of flowers shows flower counts by treatment throughout the season by each plant. This boxplot compares the number of flowers observed under (HW) or (C) treatments from the beginning (June 17,

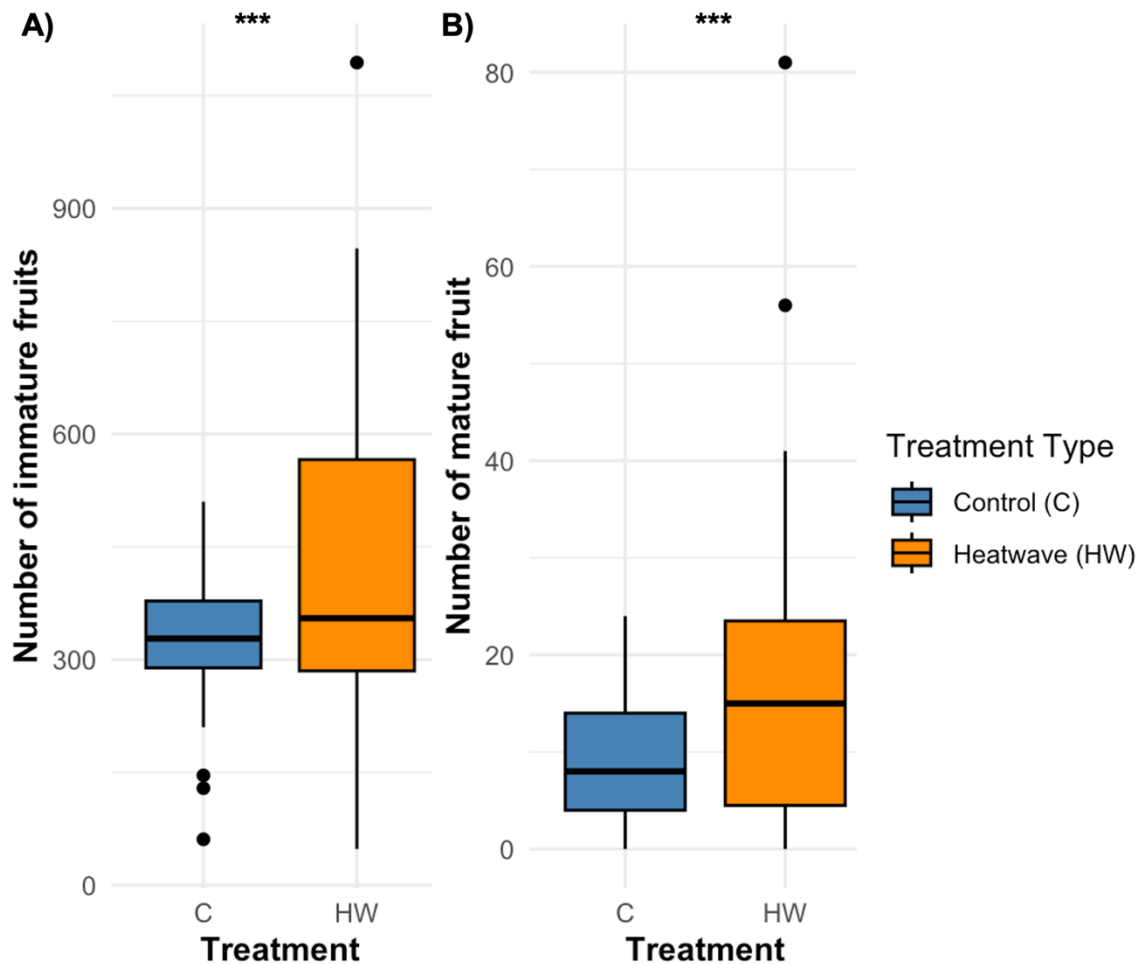
2024) to the end of the field season (August 22, 2024). To indicate statistical significance, we used (n.s) for non-significant results and (\*\*\*,  $p < 0.001$ ) for significant results.

#### **2.4.5 Fruit Production**

We found a statistically significant effect of HW treatment on immature fruit production whereby plants produced, on average, approximately 65 more immature fruits compared to the control group (Estimate = 0.240, SE = 0.01, Figure 11A). Similarly, heatwave exposure had a statistically significant effect on mature fruit production ( $\chi^2 = 104.45$ ,  $df = 1$ ,  $p = < 0.0001$ ).

Plants subjected to heatwave conditions produced, approximately 2 more mature fruits compared to the control group (Figure 11B). Excluding youth garden resulted in the same patterns ( $\chi^2 = 16.66$ ,  $df = 1$ ,  $p = < 0.001$ ). Overall, the results indicate that heatwave conditions significantly increased the production of mature and immature fruits while accounting for variability across sites.

Figure 11. Box plots of fruit production



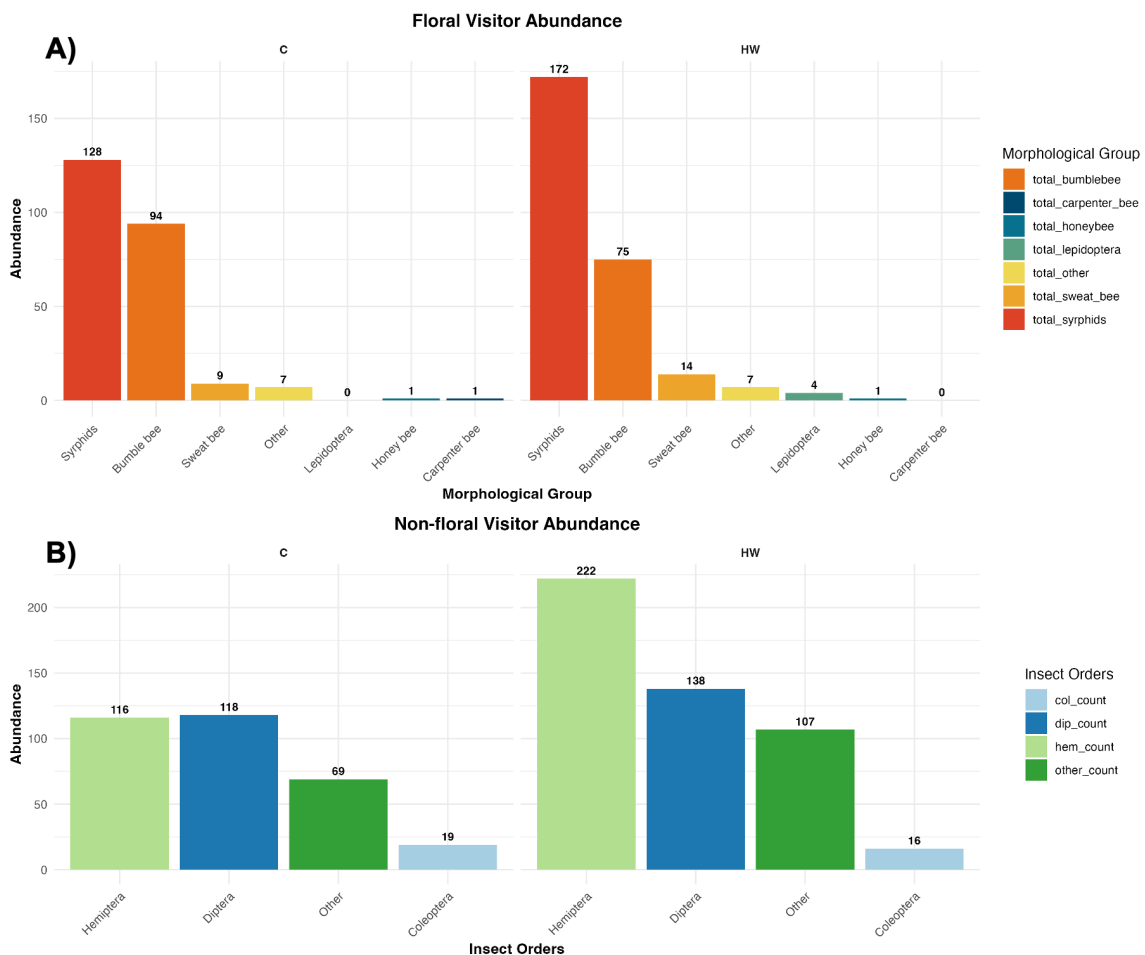
Box plots of fruit production. A) The total number of immature and B) mature fruits by treatments of heatwave (HW) or control (C) over the entire sampling period. To indicate statistical significance, we used (n.s) for non-significant results and (\*\*\*,  $p < 0.001$ ) for significant results.

#### 2.4.6 Abundance of Floral Visitors

When evaluating floral visitor abundance under controlled and heatwave conditions, the models indicated no statistically significant effect of the heatwave treatment on floral visitor abundance ( $\chi^2 = 0.0048$ ,  $df = 1$ ,  $p = 0.94$ ). Similarly, plant richness surrounding the tomato plants had no statistical effect on floral visitor abundance ( $\chi^2 = 1.85$ ,  $df = 1$ ,  $p = 0.173$ ), but was significant after youth garden exclusion ( $\chi^2 = 13.39$ ,  $df = 1$ ,  $p < 0.001$ ). To explore potential

differences in abundance among morphological groups at each site, we performed an analysis of variance (ANOVA), which revealed a significant variation in floral visitor abundance among morphological groups ( $\chi^2 = 149.84$ ,  $df = 6$ ,  $p < 0.05$ ). Post-hoc pairwise comparisons were conducted to further examine differences across morphological groups. The estimated marginal means indicated that Syrphid flies were the most abundant group, with an estimated abundance of 1.94 (95% CI: 1.13). Overall, Syrphid flies emerged as the most common group observed across sites and treatments (Figure 12A).

Figure 12. Bar plots of floral and non-floral visitors



Bar plots of floral and non-floral visitors. A) Shows the distribution of floral visitor abundance by morphological group under control (C) and heatwave (HW) conditions. Morphological group of floral visitors include syrphid flies (*total\_syrphids*), bumble bees (*total\_bumblebee*), sweat bees (*total\_sweat\_bee*), and other groups with lower abundances, such as lepidopterans (*total\_lepidoptera*), honey bees (*total\_honeybee*), and carpenter bees (*total\_car Carpenter\_bee*). B)

Shows the distribution of non-floral visitor abundance by insect orders under (C) and (HW) conditions. Non-floral visitor groups include insects the Hemiptera, Diptera, Coleoptera orders and “Other”. “Other” refers to any other insect on the plant during the survey.

#### **2.4.7 Non-floral Visitor Abundance**

Hemipterans were the most common insect order across all treatments and in the entire sampling period (Figure 12B). Treatment, surrounding plant species richness, and non-floral visitor groups (Hemiptera, Diptera, Coleoptera, and other) significantly influenced non-floral visitor abundance. The HW treatment had a strong positive effect on non-floral visitor abundance (Estimate=1.371,  $p < 0.0001$ ), indicating that the abundance of non-floral visitors under heatwave conditions is approximately 3.93 times higher than in the control group. Similarly, surrounding plant species richness had a significant positive association (Estimate = 0.33,  $p < 0.0001$ ), with each additional unit increase in surrounding plant species richness corresponding to a 38% increase in abundance.

Among the non-floral visitors, HW exposure had the strongest effect on the insect order Hemiptera (Estimate = 2.33,  $p < 0.0001$ ), suggesting a substantial increase in abundance associated with this group. Diptera also showed a significant positive effect (Estimate = 1.53,  $p < 0.0001$ ), while the other non-floral visitor groups had a smaller yet significant effect (Estimate = 0.90,  $p = 0.012$ ). Further testing showed that HW treatment ( $\chi^2 = 61.14$ ,  $df = 1$ ,  $p < 0.001$ ), surrounding plant species richness ( $\chi^2 = 57.81$ ,  $df = 1$ ,  $p < 0.001$ ), and non-floral visitor groups, including the insect orders Hemiptera, Diptera, Coleoptera and other ( $\chi^2 = 92.88$ ,  $df = 3$ ,  $p < 0.001$ ), all contributed significantly to variation in the response. These findings highlight the strong effects of heatwave treatment, species richness, and non-floral visitor abundance, particularly Hemiptera, in driving the observed patterns in the response variable.

### 2.5.1 DISCUSSION

This study explored the impact of heatwave exposure to plants on plant growth, flowering, and fruit development, as well as floral and non-floral visitors. Heatwave exposure resulted in no statistically significant differences in initial growth rate and weekly plant height. After the exclusion of youth garden, a statistically significant reduction in weekly plant height was observed under HW exposure. While there was no difference in the onset of flower bloom between treatments, HW exposure induced a delay in fruit emergence compared to the control group. The heatwave treatment had no significant effect on the number of flowers by the end of the first week, yet increased the total flower counts relative to the control. These findings highlight the complex effects of heatwave exposure on plants and the need to continue to investigate these complexities.

Heatwave exposure to plants during early development resulted in no statistically significant effects in initial growth rate. Likewise, HW exposure did not influence weekly plant height. However, after youth garden exclusion, the model showed a significant decrease in plant height. These findings align with previous research, which highlights the detrimental effects of heat stress on plant development. Studies have shown that heat stress during early growth stages disrupts key physiological processes related to flowering, reproductive success, growth, and phenology (Hasanuzzaman et al., 2013; Tun et al., 2021; Craufurd and Wheeler, 2009), which is similar to what we observed on weekly plant height after exclusion. Similarly, Tokić et al. (2023) found that heatwave exposure in *Solanum lycopersicum* plants led to a reduction in the number of roots, yellowing of leaves, stem bending, leaf wilting, and increased production of heat shock proteins that ultimately affected plant growth. It is important to emphasize that these patterns

were observed after youth garden exclusion, which shows how detrimental heatwave exposure can be for plant growth and how additional access to nutrients may serve as a mitigation strategy.

Our models for total immature and mature fruits revealed significantly higher tomato production under HW treatment, where elevated temperatures enhanced fruit yield. Despite site-specific differences in nutrient availability, the overall patterns of mature fruit production remained consistent even after exclusion. This suggests that temperature effects on fruit production were largely independent of localized nutrient conditions. These findings contrast with studies like Camejo et al. (2005), which reported that high temperatures negatively impacted photosynthetic activity, fruit development, and maturity, ultimately leading to reduced tomato yields. These results highlight the complex and context-dependent effects of heat stress on plant development, emphasizing the need for further research to understand the mechanisms driving these divergent responses.

Heatwaves delayed the development of fruits, yet did not influence flowering phenology. Understanding the effects of elevated temperatures on plant phenology is crucial, as such shifts can pose significant threats to food security and impact interactions with pollinators. For example, rising temperatures are significantly shortening the growth phases of potatoes (*Solanum tuberosum*), which are in the same genus as tomatoes (Naz et al. 2021). These findings align with our results, thus emphasizing the impact of thermal trends on crop phenology, potentially affecting productivity. Studies on other crops such as olives (*Olea europea L.*) have found similar patterns, where the exposure to higher temperatures during early development has resulted in the maturation period being forwarded and extended (Benlloch-González et al., 2019). These results highlight the importance of understanding how environmental stressors such as elevated temperature can have a significant effect on fruit ripening time.

Our study found that Syrphid flies were the most prominent floral visitors, followed by bumble bees, sweat bees, other visitors, lepidopterans, honey bees, and carpenter bees. While bees are often considered key pollinators, Syrphid flies also provide essential ecosystem services, including pollination and pest regulation, particularly in urban and diverse landscapes (Tamara et al., 2023). Although our floral visitor abundance model showed no significant differences between treatments (HW or C), it reinforced the importance of Syrphid flies as potential primary floral visitors in urban settings. Similarly, Olsson et al. (2021) demonstrated that Syrphid flies contribute significantly to plant-pollinator networks, making numerous floral visits and pollinating plant types not visited by bees. This study adds to the growing body of research recognizing the vital role of non-bee pollinators in maintaining pollination networks and supporting ecosystem health.

Even though our study showed no significance in HW exposure and floral visitor abundance, extreme heat can potentially influence pollinator behavior by altering plant attractiveness, with potential implications for pollination success (Descamps et al., 2021). In a similar study, Walters et al. (2024) examined this relationship through a no-choice field cage experiment, where blueberry (*Vaccinium corymbosum*), phacelia (*Phacelia tanacetifolia*), and white clover plants (*Trifolium repens*), respectively, were subjected to either extreme (37.5°C) or normal (25°C) temperatures during early bloom. Their findings revealed that female blue orchard bees (*Osmia lignaria*) offered heat-stressed plants laid 70% fewer eggs compared to those provided with non-stressed plants, suggesting that heat exposure makes plants less attractive to pollinators. This study presents findings that contrast with ours, highlighting the need for future research to further explore the vulnerability of plants during the early bloom stage and their interactions with pollinators, despite the differing trends observed in our results.

One of our key findings revealed a significant increase in the abundance of non-floral visitors in the HW treatment group compared to the control. Notably, insects from the order Hemiptera emerged as the dominant group. Most Hemipterans are herbivorous, and some, such as aphids, are well-known agricultural pests (Javed et al., 2024). In a related study, researchers investigated how simulated heatwaves influenced the hormone jasmonate (JA), which plays a critical role in plant resilience to various environmental stresses, including herbivore attacks, also using tomato as the model system. Their results demonstrated that herbivore-induced jasmonate signaling at elevated temperatures can block stomatal opening and leaf hyponasty, leading to leaf overheating, reduced photosynthesis, and inhibited growth (Havko et al., 2020). Furthermore, the study showed that elevated temperatures significantly increased foliage consumption of tomato plants by *Manduca sexta* in the treatment group compared to the control (Havko et al., 2020). These results further support the results of our non-floral visitor model, where it is shown the abundance of non-floral visitors is the highest in the HW group. However, it is important to note that we did not measure herbivory, and incorporating such assessments could have provided valuable additional insights.

It remains unclear whether the naturally occurring heatwave during the experimental assay influenced these observed patterns. Studies have shown that the co-occurrence of heatwaves can negatively impact plant-pollinator interactions (Siebers et al., 2015; Siebers et al., 2017; Martinet et al., 2020; Nooten et al., 2024). Siebers et al. (2015) demonstrated that repeated heatwaves over a one-year period reduced photosynthesis and increased oxidative stress, leading to significant soybean (*Glycine max*) yield losses in the U.S. Midwest. Siebers et al. (2017) found that repeated heatwaves during the reproductive stages of maize (*Zea mays*) negatively impacted reproductive biomass and decreased photosynthesis. Beyond crops, Martinet et al.

(2020) reported that simulated heatwaves affected fertility and reduced the attractiveness of male bumble bees (*Bombus terrestris*, *Bombus magnus*, and *Bombus jonellus*). Additionally, Nooten et al. (2024) observed that co-occurring heatwaves strongly reduced antennal responses to floral scents in bumble bee species (*Bombus terrestris* and *Bombus pascuorum*), disrupting critical plant-pollinator communication. These studies shine a light on the far-reaching impacts of repeated heatwaves on both plant and pollinator systems. Future research should consider evaluating repeated heatwaves regarding plant health and pollinator interactions to better understand their influence.

At one of our study sites, the HW treatment included additional access to nutrients, which may have contributed to stress alleviation. Nutrient supplementation has been shown to mitigate abiotic stresses by enhancing plant resilience (Kumari et al., 2022). Nitrogen supplementation during stress events can also increase heat tolerance by promoting chlorophyll biosynthesis, enhancing photosynthetic activity, and improving solar radiation utilization (Waraich et al., 2011; Hassan et al., 2005; Zhu et al., 2000). Similarly, potassium supplementation can help plants cope with stress by regulating stomatal function, boosting photosynthesis, and improving water uptake (Johnson et al., 2022). Youth garden exclusion resulted in a decrease in weekly plant height, suggesting that additional nutrients might have played a role in mitigating heat stress.

It is important to recognize that in a warming climate, multiple environmental stressors often occur simultaneously. In this study, however, we focused solely on evaluating our response variables in relation to elevated temperatures. As drought and heatwaves increasingly coincide (Zhou et al., 2024), understanding their combined impacts on plants remains crucial. The findings of Raja et al. (2020) highlight the significant physiological impacts of combined

drought and heat stress on tomato plants. These stressors trigger increased production of proline to help maintain cellular water balance but also lead to higher levels of reactive oxygen species, lipid peroxidation, and reduced relative water content, resulting in dehydration and potential membrane damage. The findings of Honglang et al. (2017) also demonstrate the detrimental effects of combined drought and heatwave stress on cherry tomato seedlings, significantly impairing plant growth, leaf gas exchange, and water relations. These findings highlight the significant detrimental effects that compound events, such as drought and heatwaves, can have on overall plant health. Future studies should consider assessing the effects of multiple stressors on plants, individually and combined.

Our study highlights the multifaceted impacts of simulated heatwave exposure on plant development and ecological interactions. HW exposure significantly increased the total number of immature and mature fruits. In contrast, HW exposure had no significant impact on the initial growth rate, weekly plant height, total flower production, early flowering, and floral visitor abundance. The observed increase in non-floral visitors, particularly Hemipterans, under HW conditions underscores how heat stress can influence insect populations and plant-insect dynamics. These findings contribute to our understanding of plant and insect responses to heat stress and provide valuable insights into the potential consequences of climate change for ecological and agricultural systems in urban environments. Future studies should explore the long-term and compound effects of heatwaves and other stressors to better predict and mitigate their impacts on plant health, pollination, and food security.

### **2.5.2 Strengths and Limitations of the Study**

One of the key strengths of this study is its contribution to understanding the effects of heatwave exposure during early development in urban environments, where environmental

stressors are often intensified. The study highlights the significance of non-bee floral visitors in urban ecosystems, showing their role and relevance in these settings. It lays a foundation for future research focused on developing strategies to mitigate the impacts of heat stress on ecological systems and urban agriculture.

We acknowledge that this experimental design does not include the fluctuation in day and nighttime temperatures; the temperatures were selected as extreme conditions and would benefit from complementary studies that include a range in daily maximum and range of temperature fluctuation. During the field season, plants in the heatwave group at the Youth Garden rooted through their pots, allowing them greater access to nutrients compared to plants at other sites. We analyzed the data excluding data from this site to understand how influential this confounding factor was for our results. It is important to highlight that cherry tomato fruits matured rapidly and frequently fell before measurements could be taken, which likely contributed to the discrepancy between the total number of flowers and the total number of immature and mature fruits. Our research was also restricted to three sites (Youth Garden, Holyoke Community College, and La Piedra Garden), which limits the ability to assess site-level variability. Increasing the number of study sites would enhance our ability to generalize findings and account for site-specific differences. Since our study was conducted over a single sampling season, incorporating multiple seasons in future research would provide a more comprehensive understanding of the impacts of seasonal variation in temperatures and invertebrate abundance. All study sites were located in Holyoke, Massachusetts, which may limit the generalizability of our findings. Expanding future studies to include diverse geographic locations would help capture broader environmental variability, strengthening our understanding of the ecological impacts of heatwave exposure across different urban landscapes.

## Supplementary Text

To understand the influence of excluding Youth Garden on our results, the site where HW-exposed plants had additional exposure to nutrients relative to the control, we performed all analyses including and excluding this site. Here we present the results of excluding Youth Garden from the analyses. To evaluate the effects of HW exposure on initial growth rate, flower and fruit phenology, and the total number of mature and immature fruits and flowers, we used a generalized linear mixed model (GLMM) with individual plants as the unit of replication (n=96). Treatment was included as a fixed effect, and sites were modeled as a random effect. Weekly measurements of plant height (cm) were modeled at the weekly level (n = 761) with treatment as a fixed effect and sites, individual plants, and dates as random effects. The initial number of flowers was modeled at the daily level (n = 288) with treatment as a fixed effect and individual plants as a random effect. The abundance of floral and non-floral visitors was modeled using multiple fixed effects, including treatment, plant richness, morphological groups, and non-floral visitor groups. The models included site and date as random effects. We used the same models and distributions as the models including Youth Garden to ensure proper comparison.

Heatwave exposure resulted in no statistically significant differences between treatments and initial growth rate ( $\chi^2 = 1.17$ ,  $df = 1$ ,  $p = 0.27$ ). While HW exposure resulted in a decrease in weekly plant height ( $\chi^2 = 17.65$ ,  $df = 1$ ,  $p < 0.001$ ), by an average of 5.89 cm. For our flower phenology model, HW exposure resulted in no statistically significant differences between treatments ( $\chi^2 = 0.2311$ ,  $df = 1$ ,  $p = 0.630$ ). However, HW exposure resulted in a delay in fruit phenology compared to the control group ( $\chi^2 = 110.5$ ,  $df = 1$ ,  $p < 0.001$ ). In contrast, HW exposure resulted in no statistically significant difference between treatments ( $\chi^2 = 0.093$ ,  $df = 1$ ,

p = 0.76) and initial number of flowers and the total number of flowers ( $\chi^2 = 2.21$ , df = 1, p = 0.13). Lastly, HW exposure resulted in no statistically significant differences between treatments and immature fruit production ( $\chi^2 = 0.76$ , df = 1, p = 0.383) whereas it resulted in a statistically significant difference between treatments ( $\chi^2 = 95.57$ , df = 1, p < 0.001) with HW-exposed plants producing more mature fruits than the control group.

There were no statistically significant changes between treatments and the abundance of floral visitors ( $\chi^2 = 0.0028$ , df = 1, p = 0.95). In contrast, surrounding plant species richness was significant ( $\chi^2 = 13.39$ , df = 1, p < 0.001). We also found a significant variation in floral visitor abundance among morphological groups ( $\chi^2 = 68.95$ , df = 6, p < 0.001). The non-floral visitors model showed no statistical significance between treatments ( $\chi^2 = 0.57$ , df = 1, p = 0.44) or surrounding plant species richness ( $\chi^2 = 0.0087$ , df = 1, p = 0.92), but showed statistical significance among non-floral visitor groups ( $\chi^2 = 35.22$ , df = 3, p < 0.001).

## REFERENCES

- Adamkiewicz, G., Hsu, HH., Vallarino, J. et al. Nitrogen dioxide concentrations in neighborhoods adjacent to a commercial airport: a land use regression modeling study. *Environ Health* 9, 73 (2010). <https://doi.org/10.1186/1476-069X-9-73>
- Agency for Toxic Substances and Disease Registry. Medical management guidelines for nitrogen oxides (NO, NO<sub>2</sub>, and others). Available at: <http://www.atsdr.cdc.gov/mmg/mmg.asp?id=394&tid=69>.
- Air Monitoring in Massachusetts. Mass.gov. (n.d.). <https://www.mass.gov/air-monitoring-in-massachusetts>
- Babaan, J., Wong, P., Chen, P., Chen, H., Lung, S. C., Chen, Y., & Wu, C. (2024). Geospatial artificial intelligence for estimating daytime and nighttime nitrogen dioxide concentration variations in Taiwan: A spatial prediction model. *Journal of Environmental Management*, 360, 121198. <https://doi.org/10.1016/j.jenvman.2024.121198>
- Bashir, M. A., Alvi, A. M., Khan, K. A., Rehmani, M. I. A., Ansari, M. J., Atta, S., Ghramh, H. A., Batool, T., & Tariq, M. (2017). Role of pollination in yield and physicochemical properties of tomatoes (*Lycopersicon esculentum*). *Saudi Journal of Biological Sciences*, 25(7), 1291–1297. <https://doi.org/10.1016/j.sjbs.2017.10.006>
- Benlloch-González, M., Sánchez-Lucas, R., Bejaoui, M. A., Benlloch, M., & Fernández-Escobar, R. (2019). Global warming effects on yield and fruit maturation of olive trees growing under field conditions. *Scientia Horticulturae*, 249, 162–167. <https://doi.org/10.1016/j.scienta.2019.01.046>
- Bitá C.E., Gerats T. Plant tolerance to high temperature in a changing environment: Scientific fundamentals and production of heat stress-tolerant crops. *Front. Plant Sci.* 2013;4:273. doi: 10.3389/fpls.2013.00273.
- Blaise, C., Mazzia, C., Bischoff, A. et al. Vegetation increases abundances of ground and canopy arthropods in Mediterranean vineyards. *Sci Rep* 12, 3680 (2022). <https://doi.org/10.1038/s41598-022-07529-1>
- Boningari, T., & Smirniotis, P. G. (2016). Impact of nitrogen oxides on the environment and human health: MN-based materials for the No X Abatement. *Current Opinion in Chemical Engineering*, 13, 133–141. <https://doi.org/10.1016/j.coche.2016.09.004>
- Borghini, M., De Souza, L. P., Yoshida, T., & Fernie, A. R. (2019). Flowers and climate change: a metabolic perspective. *New Phytologist*, 224(4), 1425–1441. <https://doi.org/10.1111/nph.16031>
- Bozkurt, Z., Üzmez, Ö. Ö., Döğeroğlu, T., Artun, G., & Gaga, E. O. (2018). Atmospheric concentrations of SO<sub>2</sub>, NO<sub>2</sub>, ozone and VOCs in Düzce, Turkey using passive air samplers: Sources, spatial and seasonal variations and health risk estimation. *Atmospheric Pollution Research*, 9(6), 1146–1156. <https://doi.org/10.1016/j.apr.2018.05.001>
- Cai, J., Ge, Y., Li, H., Yang, C., Liu, C., Meng, X., Wang, W., Niu, C., Kan, L., Schikowski, T., Yan, B., Chillrud, S. N., Kan, H., & Jin, L. (2020). Application of land use regression to assess exposure and identify potential sources in PM<sub>2.5</sub>, BC, NO<sub>2</sub> concentrations. *Atmospheric Environment*, 223, 117267. <https://doi.org/10.1016/j.atmosenv.2020.117267>
- Camejo, D., Rodríguez, P., Morales, M. A., Dell'Amico, J. M., Torrecillas, A., & Alarcón, J. J. (2005). High temperature effects on photosynthetic activity of two tomato cultivars with different heat susceptibility. *Journal of plant physiology*, 162(3), 281–289. <https://doi.org/10.1016/j.jplph.2004.07.014>
- Carlsaw D (2023). Worldmet: Import Surface Meteorological Data from NOAA Intergrated Surface Database (ISD)\_ . R package version 0.9.8, <https://CRAN.R-project.org/package=worldmet>

- Carslaw, D. (2005). Evidence of an increasing NO/NO emissions ratio from road traffic emissions. *Atmospheric Environment*, 39(26), 4793–4802. <https://doi.org/10.1016/j.atmosenv.2005.06.023>
- Cheeseman, M. J., Ford, B., Anenberg, S. C., Cooper, M. J., Fischer, E. V., Hammer, M. S., Magzamen, S., Martin, R. V., van Donkelaar, A., Volckens, J., & Pierce, J. R. (2022). Disparities in Air Pollutants Across Racial, Ethnic, and Poverty Groups at US Public Schools. *GeoHealth*, 6(12), e2022GH000672. <https://doi.org/10.1029/2022GH000672>
- Cheewinsiriwat, P. Estimation of nitrogen dioxide concentrations in Inner Bangkok using Land Use Regression modeling and GIS. *Appl Geomat* 8, 107–116 (2016). <https://doi.org/10.1007/s12518-016-0170-y>
- Chen, X., Qi, L., Li, S., & Duan, X. (2023). Long-term NO<sub>2</sub> exposure and mortality: A comprehensive meta-analysis. *Environmental Pollution*, 341, 122971. <https://doi.org/10.1016/j.envpol.2023.122971>
- Clark, L. P., Millet, D. B., & Marshall, J. D. (2014). National patterns in environmental injustice and inequality: outdoor NO<sub>2</sub> air pollution in the United States. *PloS one*, 9(4), e94431. <https://doi.org/10.1371/journal.pone.0094431>
- De Souza, A., De Oliveira-Júnior, J. F., Cardoso, K. R. A., & Gautam, S. (2024). Impact of vehicular emissions on ozone levels: A comprehensive study of nitric oxide and ozone interactions in urban areas. *Geosystems and Geoenvironment*, 100348. <https://doi.org/10.1016/j.geogeo.2024.100348>
- Descamps, C., Jambrek, A., Quinet, M., & Jacquemart, A. (2021). Warm temperatures reduce flower attractiveness and bumblebee foraging. *Insects*, 12(6), 493. <https://doi.org/10.3390/insects12060493>
- DOI: 10.1021/acs.est.3c03999
- Dominski, F. H., Branco, J. H. L., Buonanno, G., Stabile, L., Da Silva, M. G., & Andrade, A. (2021). Effects of air pollution on health: A mapping review of systematic reviews and meta-analyses. *Environmental Research*, 201, 111487. <https://doi.org/10.1016/j.envres.2021.111487>
- Eilers, E. J., Kremen, C., Smith Greenleaf, S., Garber, A. K., & Klein, A. M. (2011). Contribution of pollinator-mediated crops to nutrients in the human food supply. *PloS one*, 6(6), e21363. <https://doi.org/10.1371/journal.pone.0021363>
- Environmental Science & Technology 2023 57 (48), 19532-19544
- exposure to traffic-related air pollution and birth defects in Massachusetts. *Environmental research*, 146, 1–9. <https://doi.org/10.1016/j.envres.2015.12.010>
- Extreme heat safety tips*. (n.d.). Mass.gov. Retrieved May 14, 2024, from [https://www.mass.gov/info-details/extreme-heat-safety-tips?\\_gl=1\\*1ysutir\\*\\_ga\\*NjMxNTI0Nzg0LjE3MTA3MTY3MzE.\\*\\_ga\\_MCLPEGW7WM\\*MTcyNzYzNzc3NS4zLjAuMTcyNzYzNzc3NS4wLjAuMA..](https://www.mass.gov/info-details/extreme-heat-safety-tips?_gl=1*1ysutir*_ga*NjMxNTI0Nzg0LjE3MTA3MTY3MzE.*_ga_MCLPEGW7WM*MTcyNzYzNzc3NS4zLjAuMTcyNzYzNzc3NS4wLjAuMA..)
- Fiordelisi, A., Piscitelli, P., Trimarco, B., Coscioni, E., Iaccarino, G., & Sorriento, D. (2017). The mechanisms of air pollution and particulate matter in cardiovascular diseases. *Heart failure reviews*, 22(3), 337–347. <https://doi.org/10.1007/s10741-017-9606-7>
- Fisogni, A.; Rossi, M.; Sgolastra, F.; Bortolotti, L.; Bogo, G.; de Manincor, N.; Quaranta, M.; Galloni, M. Seasonal and Annual Variations in the Pollination Efficiency of a Pollinator Community of *Dictamnus Albus* L. *Plant Biology* 2016, 18 (3), 445–454.
- Fleisch, A.F., Kloog, I., Luttmann-Gibson, H. et al. Air pollution exposure and gestational diabetes mellitus among pregnant women in Massachusetts: a cohort study. *Environ Health* 15, 40 (2016). <https://doi.org/10.1186/s12940-016-0121-4>

- Flexeder, C.; Fuertes, E.; Heinrich, J.; et al. Air pollution exposure and lung function in children: The ESCAPE Project. *Environ. Health Perspect.* 2013, 121, 1357–1364.
- Foskinis, R., Gini, M. I., Kokkalis, P., Diapouli, E., Vratolis, S., Granakis, K., Zografou, O., Komppala, M., Vakkari, V., Nenes, A., Papayannis, A., & Eleftheriadis, K. (2024). On the relation between the planetary boundary layer height and in situ surface observations of atmospheric aerosol pollutants during spring in an urban area. *Atmospheric Research*, 308, 107543. <https://doi.org/10.1016/j.atmosres.2024.107543>
- Fox J, Weisberg S (2019). *An R Companion to Applied Regression*, Third edition. Sage, Thousand Oaks CA. <https://www.john-fox.ca/Companion/>
- Fox J, Weisberg S (2019). *An R Companion to Applied Regression*,
- Gaige Hunter Kerr, Daniel L. Goldberg, Maria H. Harris, Barron H. Henderson, Perry Hystad, Ananya Roy, and Susan C. Anenberg
- Gao, D., Esenther, S., Minet, L., De Jesus, A., Hudson, S., Leaderer, B., Hatzopoulou, M., & Godri Pollitt, K. J. (2023). Assessment of children's personal and land use regression model-estimated exposure to NO<sub>2</sub> in Springfield, Massachusetts. *The Science of the total environment*, 892, 164681. <https://doi.org/10.1016/j.scitotenv.2023.164681>
- George, P. E., Thakkar, N., Yasobant, S., Saxena, D., & Shah, J. (2023). Impact of ambient air pollution and socio-environmental factors on the health of children younger than 5 years in India: a population-based analysis. *The Lancet Regional Health - Southeast Asia*, 20, 100328. <https://doi.org/10.1016/j.lansea.2023.100328>
- Gérard, M.; Vanderplanck, M.; Wood, T.; Michez, D. Global Warming and Plant–Pollinator Mismatches. *Emerg. Top Life Sci.* **2020**.
- Global Pediatric Health and Equity: Solutions Exist. *International Journal of Environmental Research and Public Health*, 15(1), 16. <https://doi.org/10.3390/ijerph15010016>
- Granberry, Phillip and Valentino, Krizia, "Latinos in Massachusetts: Puerto Ricans" (2020). Gastón Institute Publications. 249. [https://scholarworks.umb.edu/gaston\\_pubs/249](https://scholarworks.umb.edu/gaston_pubs/249)
- Grant, T. L., & Wood, R. A. (2022). The influence of urban exposures and residence on childhood asthma. *Pediatric Allergy and Immunology*, 33(5). <https://doi.org/10.1111/pai.13784>
- Habeeb, D., Vargo, J. & Stone, B. Rising heatwave trends in large US cities. *Nat Hazards* **76**, 1651–1665 (2015). <https://doi.org/10.1007/s11069-014-1563-z>
- Hartig F (2024). *DHARMa: Residual Diagnostics for Hierarchical*
- Hasanuzzaman, M., Nahar, K., Alam, M. M., Roychowdhury, R., & Fujita, M. (2013). Physiological, biochemical, and molecular mechanisms of heat stress tolerance in plants. *International journal of molecular sciences*, 14(5), 9643–9684. <https://doi.org/10.3390/ijms14059643>
- Hassan M.J., Wang F., Ali S., Zhang G. Toxic effects of cadmium on rice as affected by nitrogen fertilizer form. *Plant Soil*. 2005;277:359–365. doi: 10.1007/s11104-005-8160-6.
- He, M., Zhong, Y., Chen, Y., Zhong, N., & Lai, K. (2022). Association of short-term exposure to air pollution with emergency visits for respiratory diseases in children. *iScience*, 25(9), 104879. <https://doi.org/10.1016/j.isci.2022.104879>
- Health in Cities. In: Nieuwenhuijsen, M., Khreis, H. (eds) *Integrating Human Health into Urban and Transport Planning*. Springer, Cham. [https://doi.org/10.1007/978-3-319-74983-9\\_21](https://doi.org/10.1007/978-3-319-74983-9_21)
- Heat Island impacts | US EPA. (2024, August 20). US EPA. <https://www.epa.gov/heatislands/heat-island-impacts#:~:text=Heat%20islands%20contribute%20to%20higher,and%20non%2Dfatal%20heat%20stroke>

- Hoek, G., Beelen, R., De Hoogh, K., Vienneau, D., Gulliver, J., Fischer, P., & Briggs, D. (2008). A review of land-use regression models to assess spatial variation of outdoor air pollution. *Atmospheric Environment*, 42(33), 7561–7578. <https://doi.org/10.1016/j.atmosenv.2008.05.057>
- Hoffmann, B. (2019). Air Pollution in Cities: Urban and Transport Planning Determinants and Honglang Duan, Jianping Wu, Guomin Huang, Shuangxi Zhou, Wenfei Liu, Yingchun Liao, Xue Yang, Zufe Xiao, Houbao Fan, Individual and interactive effects of drought and heat on leaf physiology of seedlings in an economically important crop, *AoB PLANTS*, Volume 9, Issue 1, January 2017, plw090, <https://doi.org/10.1093/aobpla/plw090>  
<https://CRAN.R-project.org/package=emmeans>
- Huang, S., Li, H., Wang, M., Qian, Y., Steenland, K., Caudle, W. M., Liu, Y., Sarnat, J., Papatheodorou, S., & Shi, L. (2021). Long-term exposure to nitrogen dioxide and mortality: A systematic review and meta-analysis. *The Science of the total environment*, 776, 145968. <https://doi.org/10.1016/j.scitotenv.2021.145968>
- Hwang, B.F.; Chen, Y.H.; Lin, Y.T.; Wu, X.T.; Lee, Y.L. Relationship between exposure to fine particulates and ozone and reduced lung function in children. *Environ. Res.* 2015, 137, 382–390.
- iNaturalist*. (2008). iNaturalist. Retrieved June 17, 2024, from <https://www.inaturalist.org/>
- Jackson Cote, jcote@masslive.com & Jackson Cote, jacksoncote@gmail.com. (2024, June 15). Massachusetts weather: Dangerous heat, 100-degree temps forecast next week. *Masslive*. <https://www.masslive.com/weather/2024/06/massachusetts-weather-dangerous-heat-100-degree-temps-forecast-next-week.html>
- Jarvis DJ, Adamkiewicz G, Heroux ME, et al. Nitrogen dioxide. In: WHO Guidelines for Indoor Air
- Javed, K., Smagghe, G., Hussain, B. *et al.* Exploring innovative strategies to control aphids: meta-analysis and a critical view on what we have and what the future is. *J Pest Sci* (2024). <https://doi.org/10.1007/s10340-024-01852-4>
- Jiang, Q., Mei, D., & Feng, D. (2016). Air pollution and chronic airway diseases: What should people know and do? *Journal of Thoracic Disease*, 8(1), E31. <https://doi.org/10.3978/j.issn.2072-1439.2015.11.50>
- Johnson, R., Vishwakarma, K., Hossen, M. S., Kumar, V., Shackira, A., Puthur, J. T., Abdi, G., Sarraf, M., & Hasanuzzaman, M. (2022). Potassium in plants: Growth regulation, signaling, and environmental stress tolerance. *Plant Physiology and Biochemistry*, 172, 56–69. <https://doi.org/10.1016/j.plaphy.2022.01.001>
- Kazemiparkouhi, F., Eum, K.-D., Wang, B., Manjourides, J., & Suh, H. H. (2019a). Long-term ozone exposures and cause-specific mortality in a US medicare cohort. *Journal of Exposure Science & Environmental Epidemiology*, 30(4), 650–658. <https://doi.org/10.1038/s41370-019-0135-4>
- Kendrick, C. M., Koonce, P., & George, L. A. (2015). Diurnal and seasonal variations of NO, NO<sub>2</sub> and PM<sub>2.5</sub> mass as a function of traffic volumes alongside an urban arterial. *Atmospheric Environment*, 122, 133–141. <https://doi.org/10.1016/j.atmosenv.2015.09.019>
- Keshavarzian, E., Kwok, K. C., Dong, K., Chauhan, K., & Zhang, Y. (2022). An experimental investigation of stagnant air pollution dispersion around a building in a turbulent flow. *Building and Environment*, 224, 109564. <https://doi.org/10.1016/j.buildenv.2022.109564>
- Landrigan, P.J., Fisher, S., Kenny, M.E. et al. A replicable strategy for mapping air pollution’s community-level health impacts and catalyzing prevention. *Environ Health* 21, 70 (2022). <https://doi.org/10.1186/s12940-022-00879-3>

- Larkin, A., Anenberg, S., Goldberg, D. L., Mohegh, A., Brauer, M., & Hystad, P. (2023). A global spatial-temporal land use regression model for nitrogen dioxide air pollution. *Frontiers in Environmental Science*, 11. <https://doi.org/10.3389/fenvs.2023.1125979>
- Larkin, A., Geddes, J. A., Martin, R. V., Xiao, Q., Liu, Y., Marshall, J. D., Brauer, M., & Hystad, P. (2017). Global Land Use Regression Model for Nitrogen dioxide Air Pollution. *Environmental Science & Technology*, 51(12), 6957–6964. <https://doi.org/10.1021/acs.est.7b01148>
- Lenth R (2024). *\_emmeans: Estimated Marginal Means, aka Least-Squares Means\_*. R package version 1.10.5,
- Link to NSRT\_mk3 protocol: [https://www.instrumentchoice.com.au/sound-level-meter-data-logger-with-type-1-microphone-ic-nsrt\\_mk3#description](https://www.instrumentchoice.com.au/sound-level-meter-data-logger-with-type-1-microphone-ic-nsrt_mk3#description)
- Mananga ES, Lopez E, Diop A, Dongomale PJ, Diane F. The impact of the air pollution on health in New York City. *Journal of Public Health Research*. 2023;12(4). doi:[10.1177/22799036231205870](https://doi.org/10.1177/22799036231205870)
- Marcelo A. Aizen, Lucas A. Garibaldi, Saul A. Cunningham, Alexandra M. Klein, How much does agriculture depend on pollinators? Lessons from long-term trends in crop production, *Annals of Botany*, Volume 103, Issue 9, June 2009, Pages 1579–1588, <https://doi.org/10.1093/aob/mcp076>
- Martinet, B., Zambra, E., Przybyla, K., Lecocq, T., Anselmo, A., Nonclercq, D., Rasmont, P., Michez, D., & Hennebert, E. (2020). Mating under climate change: Impact of simulated heatwaves on the reproduction of model pollinators. *Functional Ecology*, 35(3), 739–752. <https://doi.org/10.1111/1365-2435.13738>
- Massachusetts 2022 Air Quality Report. (n.d.). <https://www.mass.gov/doc/2022-annual-ambient-air-quality-monitoring-network-plan/download>
- Massachusetts Association of Community Development Corporations (MACCDC). (2023). (rep.). *Advancing Housing Quality and Health Equity in Massachusetts: A Path Toward Addressing Lead Paint and Indoor Air Quality*.
- Matthaios, V. N., Harrison, R. M., Koutrakis, P., & Bloss, W. J. (2023). In-vehicle exposure to NO<sub>2</sub> and PM<sub>2.5</sub>: A comprehensive assessment of controlling parameters and reduction strategies to minimise personal exposure. *The Science of the Total Environment*, 900, 165537. <https://doi.org/10.1016/j.scitotenv.2023.165537>
- Mavko, M. E., Tang, B., & George, L. A. (2008). A sub-neighborhood scale land use regression model for predicting NO<sub>2</sub>. *The Science of the Total Environment*, 398(1–3), 68–75. <https://doi.org/10.1016/j.scitotenv.2008.02.017>
- McIntyre, A., Heidari, L., Hagen, M., Bongiovanni, R., Bowman, B. N., Fabian, P., Kinney, P., & Scammell, M. K. (2024). Extreme heat and Air quality: Community Leader Perspectives on information barriers and opportunities in two environmental justice communities. *NEW SOLUTIONS a Journal of Environmental and Occupational Health Policy*. <https://doi.org/10.1177/10482911241290557>
- Mishra, S., Spaccarotella, K., Gido, J., Samanta, I., & Chowdhary, G. (2023). Effects of Heat Stress on Plant-Nutrient Relations: An Update on Nutrient Uptake, Transport, and Assimilation. *International journal of molecular sciences*, 24(21), 15670. <https://doi.org/10.3390/ij>
- Mollie E. Brooks, Kasper Kristensen, Koen J. van Benthem, Arni Magnusson, Casper W. Berg, Anders Nielsen, Hans J. Skaug, Martin Maecheler and Benjamin M. Bolker (2017). *glmmTMB Balances Speed and Flexibility Among Packages for Zero-inflated Generalized Linear Mixed Modeling*. *The R Journal*, 9(2), 378-400. doi: 10.32614/RJ-2017-066.
- Moore, K., Neugebauer, R., Lurmann, F., Hall, J., Brajer, V., Alcorn, S., & Tager, I. (2008). Ambient Ozone Concentrations Cause Increased Hospitalizations for Asthma in Children: An 18-Year

- Study in Southern California. *Environmental Health Perspectives*, 116(8), 1063-1070. <https://doi.org/10.1289/ehp.10497>
- Moriarty, P., & Honnery, D. (2014). Future cities in a warming world. *Futures*, 66, 45–53. <https://doi.org/10.1016/j.futures.2014.12.009>
- Murphy, K. J., Alpert, P., & Cosentino, D. (1999). Local impacts of a rural coal-burning generating station on lichen abundance in a New England forest. *Environmental Pollution*, 105(3), 349–354. [https://doi.org/10.1016/s0269-7491\(99\)00043-3](https://doi.org/10.1016/s0269-7491(99)00043-3)
- N.E. Havko, M.R. Das, A.M. McClain, G. Kapali, T.D. Sharkey, G.A. Howe, Insect herbivory antagonizes leaf cooling responses to elevated temperature in tomato, *Proc. Natl. Acad. Sci. U.S.A.*
- NAAQS Table | US EPA. (2024b, December 16). US EPA. <https://www.epa.gov/criteria-air-pollutants/naaqs-table>
- National Research Council (US) Subcommittee on Rocket-Emission Toxicants. Assessment of Exposure-Response Functions for Rocket-Emission Toxicants. Washington (DC): National Academies Press (US); 1998. Appendix E, ACUTE TOXICITY OF NITROGEN DIOXIDE. Available from: <https://www.ncbi.nlm.nih.gov/books/NBK230446/>
- Naz, S., Ahmad, S., Abbas, G., Fatima, Z., Hussain, S., Ahmed, M., Khan, M. A., Khan, A., Fahad, S., Nasim, W., Ercisli, S., Wilkerson, C. J., & Hoogenboom, G. (2021). Modeling the impact of climate warming on potato phenology. *European Journal of Agronomy*, 132, 126404. <https://doi.org/10.1016/j.eja.2021.126404>
- Neumann, A. E., Conitz, F., Karleowski, S., Sturm, U., Schmack, J. M., & Egerer, M. (2024). Flower richness is key to pollinator abundance: the role of garden features in cities. *Basic and Applied Ecology*. <https://doi.org/10.1016/j.baae.2024.06.004>
- Nguyen, D., Lin, C., Vu, C., Cheruiyot, N. K., Nguyen, M. K., Le, T. H., Lukkhasorn, W., Vo, T., & Bui, X. (2022b). Tropospheric ozone and NOx: A review of worldwide variation and meteorological influences. *Environmental Technology & Innovation*, 28, 102809. <https://doi.org/10.1016/j.eti.2022.102809>
- Nih chapter on Nitrogen Dioxide
- NOAA's National Weather Service. (n.d.). *Climate*. <https://www.weather.gov/wrh/Climate?wfo=box>
- Nooten, S. S., Korten, H., Schmitt, T., & Kárpáti, Z. (2024). The heat is on: reduced detection of floral scents after heatwaves in bumblebees. *Proceedings of the Royal Society B Biological Sciences*, 291(2029). <https://doi.org/10.1098/rspb.2024.0352>
- Olsson, R. L., Brousil, M. R., Clark, R. E., Baine, Q., & Crowder, D. W. (2021). Interactions between plants and pollinators across urban and rural farming landscapes. *Food Webs*, 27, e00194. <https://doi.org/10.1016/j.fooweb.2021.e00194>
- Osman, M. a. M., & Shebl, M. A. (2020). Vulnerability of crop pollination ecosystem services to climate change. In Springer water (pp. 223–247). [https://doi.org/10.1007/978-3-030-41629-4\\_11](https://doi.org/10.1007/978-3-030-41629-4_11)
- Ozgen, S., Cernuschi, S., & Caserini, S. (2020). An overview of nitrogen oxides emissions from biomass combustion for domestic heat production. *Renewable and Sustainable Energy Reviews*, 135, 110113. <https://doi.org/10.1016/j.rser.2020.110113>
- Pandey, B., & Ghosh, A. (2023). Urban ecosystem services and climate change: a dynamic interplay. *Frontiers in Sustainable Cities*, 5. <https://doi.org/10.3389/frsc.2023.1281430>
- Perera, F. (2017). Pollution from fossil-fuel combustion is the leading environmental threat to
- Perkins-Kirkpatrick, S.E., Lewis, S.C. Increasing trends in regional heatwaves. *Nat Commun* 11, 3357 (2020). <https://doi.org/10.1038/s41467-020-16970-7>

- Petit, Priscilla C.\*; Fine, David H.\*; Vásquez, Gregory B.\*; Gamero, Lucas\*; Slaughter, Mark S.†; Dasse, Kurt A.\*. The Pathophysiology of Nitrogen Dioxide During Inhaled Nitric Oxide Therapy. *ASAIO Journal* 63(1):p 7-13, January/February 2017. | DOI: 10.1097/MAT.0000000000000425
- Prather, C. M., Pelini, S. L., Laws, A., Rivest, E., Woltz, M., Bloch, C. P., Del Toro, I., Ho, C., Kominoski, J., Newbold, T. a. S., Parsons, S., & Joern, A. (2012). Invertebrates, ecosystem services and climate change. *Biological Reviews/Biological Reviews of the Cambridge Philosophical Society*, 88(2), 327–348. <https://doi.org/10.1111/brv.12002>
- Prathibha, P., Yeager, R., Bhatnagar, A., & Turner, J. (2023). Green Heart Louisville: intra-urban, hyperlocal land-use regression modeling of nitrogen oxides and ozone. medRxiv : the preprint server for health sciences, 2023.03.03.23286765. <https://doi.org/10.1101/2023.03.03.23286765>
- Prestby, Timothy J et al. 2023. “Characterizing user needs for Beescape: A spatial decision support tool focused on pollinator health.” *Journal of Environmental Management* 325: 116416. <https://doi.org/10.1016/j.jenvman.2022.116416>.
- Pun, V. C., Yu, I. T., Qiu, H., Ho, K., Sun, Z., Louie, P. K., Wong, T. W., & Tian, L. (2014). Short-Term Associations of Cause-Specific Emergency Hospitalizations and Particulate Matter Chemical Components in Hong Kong. *American Journal of Epidemiology*, 179(9), 1086-1095. <https://doi.org/10.1093/aje/kwu026>
- Qian, Y., Li, H., Rosenberg, A., Li, Q., Sarnat, J., Papatheodorou, S., Schwartz, J., Liang, D., Liu, Y., Liu, P., & Shi, L. (2021). Long-Term Exposure to Low-Level NO<sub>2</sub> and Mortality among the Elderly Population in the Southeastern United States. *Environmental health perspectives*, 129(12), 127009. <https://doi.org/10.1289/EHP9044>
- Quality: Selected Pollutants. Geneva: World Health Organization; 2010. 5. Available from: <https://www.ncbi.nlm.nih.gov/books/NBK138707/>.
- R Core Team (2021). R: A language and environment for statistical computing. R Foundation for Statistical Computing, Vienna, Austria. URL <https://www.R-project.org/>.
- Rafferty, N. E., & Ives, A. R. (2010). Effects of experimental shifts in flowering phenology on plant-pollinator interactions. *Ecology Letters*, 14(1), 69–74. <https://doi.org/10.1111/j.1461-0248.2010.01557.x>
- Raja, V., Qadir, S. U., Alyemeni, M. N., & Ahmad, P. (2020). Impact of drought and heat stress individually and in combination on physio-biochemical parameters, antioxidant responses, and gene expression in *Solanum lycopersicum*. *3 Biotech*, 10(5), 208. <https://doi.org/10.1007/s13205-020-02206-4>
- Richardson, M. L., & Arlotta, C. G. (2022). Producing Cherry Tomatoes in Urban Agriculture. *Horticulturae*, 8(4), 274. <https://doi.org/10.3390/horticulturae8040274>
- Rivas I, Viana M, Moreno T, Pandolfi M, Amato F, Reche C, Bouso L, Álvarez-Pedrerol M, Roberts–Semple, D., Song, F., & Gao, Y. (2012). Seasonal characteristics of ambient nitrogen oxides and ground–level ozone in metropolitan northeastern New Jersey. *Atmospheric Pollution Research*, 3(2), 247–257. <https://doi.org/10.5094/apr.2012.027>
- Román-Cascón, C., Yagüe, C., Ortiz-Corral, P., Serrano, E., Sánchez, B., Sastre, M., Maqueda, G., Alonso-Blanco, E., Artiñano, B., Gómez-Moreno, F., Diaz-Ramiro, E., Fernández, J., Martilli, A., García, A., Núñez, A., Cordero, J., Narros, A., & Borge, R. (2023). Wind and turbulence relationship with NO<sub>2</sub> in an urban environment: a fine-scale observational analysis. *Urban Climate*, 51, 101663. <https://doi.org/10.1016/j.uclim.2023.101663>

- Rosofsky, A., Levy, J., Zanobetti, A., Janulewicz, P., & Fabian, M. (2018). Temporal trends in air pollution exposure inequality in Massachusetts. *Environmental Research*, 161, 76–86. <https://doi.org/10.1016/j.envres.2017.10.028>
- Salonen, H., Salthammer, T., & Morawska, L. (2019). Human exposure to NO<sub>2</sub> in school and office indoor environments. *Environment International*, 130, 104887. <https://doi.org/10.1016/j.envint.2019.05.081>
- Shen, W., Ming, Y., Zhu, T., & Luo, L. (2023). The association between air pollutants and hospitalizations for asthma: an evidence from Chengdu, China. *Annals of translational medicine*, 11(2), 65. <https://doi.org/10.21037/atm-22-6265>
- Siebers, M. H., Slattery, R. A., Yendrek, C. R., Locke, A. M., Drag, D., Ainsworth, E. A., Bernacchi, C. J., & Ort, D. R. (2017). Simulated heat waves during maize reproductive stages alter reproductive growth but have no lasting effect when applied during vegetative stages. *Agriculture Ecosystems & Environment*, 240, 162–170. <https://doi.org/10.1016/j.agee.2016.11.008>
- Siebers, M. H., Yendrek, C. R., Drag, D., Locke, A. M., Acosta, L. R., Leakey, A. D. B., Ainsworth, E. A., Bernacchi, C. J., & Ort, D. R. (2015). Heat waves imposed during early pod development in soybean (*Glycine max*) cause significant yield loss despite a rapid recovery from oxidative stress. *Global Change Biology*, 21(8), 3114–3125. <https://doi.org/10.1111/gcb.12935>
- Smith, A., Sheppard, T., Burkott, J., Twohig, J., Larossi, M., Stokes, N., & Wojtowicz, E. (2013, February 6). City of Holyoke: Open Space and Recreation Plan. <https://web.archive.org/web/20170201122559/https://www.holyoke.org/wp-content/uploads/2012/10/reducedfinal2.pdf>
- Strahan, D. (2019, April 17). Paper Mills, Holyoke, Mass. Lost New England. <https://lostnewengland.com/2019/04/paper-mills-holyoke-mass-2/>
- Tamara, M. E. L., Latty, T., Threlfall, C. G., Young, A., & Hochuli, D. F. (2023). Responses of hover fly diversity and abundance to urbanisation and local attributes of urban greenspaces. *Basic and Applied Ecology*, 70, 12–26. <https://doi.org/10.1016/j.baae.2023.04.002>
- Terry, B., Kremer, P., Goldsmith, S. T., & Shakya, K. M. (2024). Land use regression model to predict nitrogen dioxide in the greater Philadelphia area. *Atmospheric Pollution Research*, 102339. <https://doi.org/10.1016/j.apr.2024.102339>
- The United States Geological Survey Landsat Normalized Difference Vegetation Index. 2020. (available at: <https://www.usgs.gov/landsat-missions/landsat-normalized-difference-vegetation-index>)
- Tokić, M., Levanić, D. L., Ludwig-Müller, J., & Bauer, N. (2023). Growth and molecular responses of tomato to Prolonged and Short-Term Heat Exposure. *International Journal of Molecular Sciences*, 24(5), 4456. <https://doi.org/10.3390/ijms24054456>
- Trunschke, J., Junker, R.R., Kudo, G. et al. Effects of climate change on plant-pollinator interactions and its multitrophic consequences. *Alp Botany* 134, 115–121 (2024). <https://doi.org/10.1007/s00035-024-00316-w>
- Tu, R., Xu, J., Wang, A., Zhai, Z., & Hatzopoulou, M. (2020). Effects of ambient temperature and cold starts on excess NO<sub>x</sub> emissions in a gasoline direct injection vehicle. *The Science of the Total Environment*, 760, 143402. <https://doi.org/10.1016/j.scitotenv.2020.143402>
- Tun, W., Yoon, J., Jeon, J., & An, G. (2021). Influence of climate change on flowering time. *Journal of Plant Biology*, 64(3), 193–203. <https://doi.org/10.1007/s12374-021-09300-x>
- U.S Census Bureau quickfacts: Holyoke City, Massachusetts. (n.d.-b). <https://www.census.gov/quickfacts/fact/table/holyokecitymassachusetts/PST045222>
- US EPA, 2021a. Overview of EPA’s Motor Vehicle Emission Simulator (MOVES3)

- USGCRP, Sarofim, M., Habeeb, D., Kunkel, K., & Kunkel, K. (2017). *Technical documentation: Heat Waves*. [https://www.epa.gov/sites/default/files/2021-04/documents/heat-waves\\_td.pdf](https://www.epa.gov/sites/default/files/2021-04/documents/heat-waves_td.pdf)
- Vasiliev, D., & Greenwood, S. (2021). The role of climate change in pollinator decline across the Northern Hemisphere is underestimated. *The Science of the Total Environment*, 775, 145788. <https://doi.org/10.1016/j.scitotenv.2021.145788>
- Walters, J., Barlass, M., Fisher, R., & Isaacs, R. (2024). Extreme heat exposure of host plants indirectly reduces solitary bee fecundity and survival. *Proceedings of the Royal Society B Biological Sciences*, 291(2025). <https://doi.org/10.1098/rspb.2024.0714>
- Wang, C., Li, Z., Chen, Y., Ouyang, L., Li, Y., Sun, F., Liu, Y., & Zhu, J. (2023). Drought-heatwave compound events are stronger in drylands. *Weather and Climate Extremes*, 42, 100632. <https://doi.org/10.1016/j.wace.2023.100632>
- Wang, J., Alli, A. S., Clark, S. N., Ezzati, M., Brauer, M., Hughes, A. F., Nimo, J., Moses, J. B., Baah, S., Nathvani, R., D, V., Agyei-Mensah, S., Baumgartner, J., Bennett, J. E., & Arku, R. E. (2024). Inequalities in urban air pollution in sub-Saharan Africa: an empirical modeling of ambient NO and NO<sub>2</sub> concentrations in Accra, Ghana. *Environmental research letters : ERL* [Web site], 19(3), 034036. <https://doi.org/10.1088/1748-9326/ad2892>
- Wang, M., Li, H., Huang, S., Qian, Y., Steenland, K., Xie, Y., Papatheodorou, S., & Shi, L. (2021). Short-term exposure to nitrogen dioxide and mortality: A systematic review and meta-analysis. *Environmental research*, 202, 111766. <https://doi.org/10.1016/j.envres.2021.111766>
- Wang, Y., Liu, P., Schwartz, J., Castro, E., Wang, W., Chang, H., Scovronick, N., & Shi, L. (2023). Disparities in ambient nitrogen dioxide pollution in the United States. *Proceedings of the National Academy of Sciences*, 120(16). <https://doi.org/10.1073/pnas.2208450120>
- Waraich E.A., Ahmad R., Ashraf M.Y., Saifullah Ahmad M. Improving agricultural water use efficiency by nutrient management in crop plants. *Acta Agric. Scand. B Soil. Plant Sci.* 2011;61:291–304. doi: 10.1080/09064710.2010.491954.
- Wickham H, Francois R, Henry L, Muller K, Vaughan D (2023). *dplyr: A Grammar of Data Manipulation*. R package version 1.1.4, <https://CRAN.R-project.org/package=dplyr>
- World Health Organization: WHO. (2021, September 22). What are the WHO Air quality guidelines? <https://www.who.int/news-room/feature-stories/detail/what-are-the-who-air-quality-guidelines>
- World Health Organization. (n.d.). Household air pollution. World Health Organization. <https://www.who.int/news-room/fact-sheets/detail/household-air-pollution-and-health#:~:text=Household%20air%20pollution%20was%20responsible,6.7%20million%20premature%20deaths%20annually.>
- Zhang, J. (Jim), Wei, Y., & Fang, Z. (2019). Ozone pollution: A major health hazard worldwide. *Frontiers in Immunology*, 10. <https://doi.org/10.3389/fimmu.2019.02518>
- Zhanqing Li, Jianping Guo, Aijun Ding, Hong Liao, Jianjun Liu, Yele Sun, Tijian Wang, Huiwen Xue, Hongsheng Zhang, Bin Zhu, Aerosol and boundary-layer interactions and impact on air quality, *National Science Review*, Volume 4, Issue 6, November 2017, Pages 810–833, <https://doi.org/10.1093/nsr/nwx117>
- Zhou, S., Wu, S., Gao, J., Liu, L., Li, D., Yan, R., & Wang, J. (2024). Increased stress from compound drought and heat events on vegetation. *The Science of the Total Environment*, 949, 175113. <https://doi.org/10.1016/j.scitotenv.2024.175113>
- Zhu Z., Gerendas J., Bendixen R., Schinner K., Tabrizi H., Sattelmacher B., Hansen U.P. Different tolerance to light stress in N<sub>03</sub>--and NH<sub>4</sub><sup>+</sup>-grown *Phaseolus vulgaris* L. *Plant Biol.* 2000;2:558–570. doi: 10.1055/s-2000-7498.